more selectively accumulate and retain longer in various tumor xenografts transplanted s.c. compared with CPT-11 (15–17). In the present study, we succeeded in demonstrating higher accumulation and longer retention of NK012 compared with CPT-11 in orthotopic and peritoneal disseminated gastric cancer model that is closer to human gastric cancer in clinics.

Peritoneal dissemination sometimes causes intestinal obstruction, which enhances the enterohepatic circulation of SN-38 after direct damage to the small intestine, and makes the use of CPT-11 difficult (26, 27). In the present study, no mouse in the NK012 group developed diarrhea. The dose-limiting toxic effects of CPT-11 seem to be neutropenia and diarrhea. In our previous data, however, there was no significant difference in the level of SN-38 in the small intestine between mice treated with NK012 and mice treated with CPT-11 despite the higher plasma area under the concentration of NK012 than CPT-11 (15). Moreover, no serious diarrhea has been reported even at the MTD dose in two phase I clinical trials against advanced solid tumors in Japan and the US (28, 29).

In conclusion, we showed that NK012 exerts significantly more potent antitumor activity against peritoneal dissemination of scirrhous gastric cancer cells than CPT-11, indicating the possibility of the clinical evaluation of this drug in patients with disseminated grastic cancer.

Disclosure of Potential Conflicts of Interest

No potential conflicts of interest were disclosed.

Acknowledgments

Received 7/23/2008; revised 9/2/2008; accepted 9/16/2008.

Grant support: Third Term Comprehensive Contorol Research for Cancer from the Ministry of Health, Labor and Welfare of Japan (Y. Matsumura) and a Grant-in-Aid for Scientific Research on Priority Areas from the Ministry of Education, Culture, Sports, Science and Technology (Y. Matsumura).

The costs of publication of this article were defrayed in part by the payment of page charges. This article must therefore be hereby marked *advertisement* in accordance with 18 U.S.C. Section 1734 solely to indicate this fact.

References

1. Koizumi W, Narahara H, Hara T, et al. S-1 plus cisplatin versus S-1 alone for first-line treatment of advanced gastric cancer (SPIRITS trial): a phase III trial. Lancet Oncol 2008;9:215–21.
2. Maehara Y, Moriguchi S, Orita H, et al. Lower survival rate for patients with carcinoma of the stomach of Borrmann type IV after gastric resection. Surg Gynecol Obstet 1992;175:13–6.
3. Yonemura Y. Mechanisms of drug resistance in gastric cancer. In: Yonemura Y, editor. Contemporary Approaches Toward Cure of Gastric Cancer. Kanazawa: Maeda Shoten Co. Ltd.; 1996. p. 87–91.
4. Yashiro M, Chung YS, Nishimura S, Inoue T, Sowa M. Fibrosis in the peritoneum induced by scirrhous gastric cancer cells may act as "soil" for peritoneal dissemination. Cancer 1996;77:1668–75.
5. Jain RK. Barriers to drug delivery in solid tumors. Sci Am 1994;271:58–65.
6. Senger DR, Galli SJ, Dvorak AM, Perruzzi CA, Harvey VS, Dvorak HF. Tumor cells secrete a vascular permeability factor that promotes accumulation of ascites fluid. Science 1983;219:983–5.
7. Dvorak HF, Brown LF, Detmar M, Dvorak AM. Vascular permeability factor/vascular endothelial growth factor, microvascular hyperpermeability, and angiogenesis. Am J Pathol 1995;146:1029–39.
8. Nagy JA, Masse EM, Herzberg KT, et al. Pathogenesis of ascites tumor growth: vascular permeability factor, vascular hyperpermeability, and ascites fluid accumulation. Cancer Res 1995;55:360–8.
9. Boocock CA, Charnock-Jones DS, Sharkey AM, et al. Expression of vascular endothelial growth factor and its receptors flt and KDR in ovarian carcinoma. J Natl Cancer Inst 1995;87:506–16.
10. Aoyagi K, Kouhuji K, Yano S, et al. VEGF significance in peritoneal recurrence from gastric cancer. Gastric Cancer 2005;8:155–63.
11. Maeda H, Matsumura Y, Kato H. Purification and identification of [hydroxyprolyl3]bradykinin in ascitic fluid from a patient with gastric cancer. J Biol Chem 1988;263:16051–4.
12. Matusmura Y, Maruo K, Kimura M, Yamamoto T, Konno T, Maeda H. Kinin-generating cascade in advanced cancer patients and *in vitro* study. Jpn J Cancer Res 1991;82:732–41.
13. Wu J, Akaike T, Hayashida K, et al. Identification of bradykinin receptors in clinical cancer specimens and murine tumor tissues. Int J Cancer 2002;98:29–35.
14. Matsumura Y, Maeda H. A new concept for macromolecular therapeutics in cancer chemotherapy: mechanism of tumoritropic accumulation of proteins and the antitumor agent smancs. Cancer Res 1986;46:6387–92.
15. Koizumi F, Kitagawa M, Negishi T, et al. Novel SN-38-incorporating polymeric micelles, NK012, eradicate vascular endothelial growth factor-secreting bulky tumors. Cancer Res 2006;66:10048–56.
16. Nakajima TE, Yasunaga M, Kano Y, et al. Synergistic antitumor activity of the novel SN-38-incorporating polymeric micelles, NK012, combined with 5-fluorouracil in a mouse model of colorectal cancer, as compared with that of irinotecan plus 5-fluorouracil. Int J Cancer 2008;122:2148–53.
17. Saito Y, Yasunaga M, Kuroda J, Koga Y, Matsumura Y. Enhanced distribution of NK012, a polymeric micelle-encapsulated SN-38, and sustained release of SN-38 within tumors can beat a hypovascular tumor. Cancer Sci 2008;99:1258–64.
18. Yanagihara K, Takigahira M, Tanaka H, et al. Development and biological analysis of peritoneal metastasis mouse models for human scirrhous stomach cancer. Cancer Sci 2005;96:323–32.
19. Yanagihara K, Takigahira M, Takeshita F, et al. A photon counting technique for quantitatively evaluating progression of peritoneal tumor dissemination. Cancer Res 2006;66:7532–9.
20. Yanagihara K, Tanaka H, Takigahira M, et al. Establishment of two cell lines from human gastric scirrhous carcinoma that possess the potential to metastasize spontaneously in nude mice. Cancer Sci 2004;95:575–82.
21. Arao T, Yanagihara K, Takigahira M, et al. ZD6474 inhibits tumor growth and intraperitoneal dissemination in a highly metastatic orthotopic gastric cancer model. Int J Cancer 2006;118:483–9.
22. Slatter JG, Schaaf LJ, Sams JP, et al. Pharmacokinetics, metabolism, and excretion of irinotecan (CPT-11) following I.V. infusion of [(14)C]CPT-11 in cancer patients. Drug Metab Dispos 2000;28:423–33.
23. Rothenberg ML, Kuhn JG, Burris HA III, et al. Phase I and pharmacokinetic trial of weekly CPT-11. J Clin Oncol 1993;11:2194–204.
24. Guichard S, Terret C, Hennebelle I, et al. CPT-11 converting carboxylesterase and topoisomerase activities in tumour and normal colon and liver tissues. Br J Cancer 1999;80:364–70.
25. Kawato Y, Aonuma M, Hirota Y, Kuga H, Sato K. Intracellular roles of SN-38, a metabolite of the camptothecin derivative CPT-11, in the antitumor effect of CPT-11. Cancer Res 1991;51:4187–91.
26. Araki E, Ishikawa M, Iigo M, Koide T, Itabashi M, Hoshi A. Relationship between development of diarrhea and the concentration of SN-38, an active metabolite of athymic mice following intraperitoneal administration of CPT-11. Jpn J Cancer Res 1993;84:697–702.
27. Atsumi R, Suzuki W, Hakusui H. Identification of the metabolites of irinotecan, a new derivative of camptothecin, in rat bile and its biliary excretion. Xenobiotica 1991;21:1159–69.
28. Kato K, Hamaguchi T, Shirao K, et al. Interim analysis of phase I study of NK012, polymer micelle SN-38, in patients with advanced cancer. Proc Am Soc Clin Oncol GI 2008 (Abs #485).
29. Burris HA III, Infante JR, Spigel DR, et al. A phase I dose-escalation study of NK012. Proc Am Soc Clin Oncol 2008 (Abs #2358).

Novel SN-38–Incorporated Polymeric Micelle, NK012, Strongly Suppresses Renal Cancer Progression

Makoto Sumitomo,[1] Fumiaki Koizumi,[2] Takako Asano,[1] Akio Horiguchi,[1] Keiichi Ito,[1] Tomohiko Asano,[1] Tadao Kakizoe,[3] Masamichi Hayakawa,[1] and Yasuhiro Matsumura[4]

[1]Department of Urology, National Defense Medical College, Tokorozawa, Saitama, Japan; [2]Shien-Lab, Medical Oncology, National Cancer Center Hospital; [3]National Cancer Center, Tokyo, Japan; and [4]Investigative Treatment Division, Research Center for Innovative Oncology, National Cancer Center Hospital East, Chiba, Japan

Abstract

It has been recently reported that NK012, a 7-ethyl-10-hydroxy-camptothecin (SN-38)–releasing nanodevice, markedly enhances the antitumor activity of SN-38, especially in hypervascular tumors through the enhanced permeability and retention effect. Renal cell carcinoma (RCC) is a typical hypervascular tumor with an irregular vascular architecture. We therefore investigated the antitumor activity of NK012 in a hypervascular tumor model from RCC. Immunohistochemical examination revealed that Renca tumors contained much more CD34-positive neovessels than SKRC-49 tumors. Compared with CPT-11, NK012 had significant antitumor activity against both bulky Renca and SKRC-49 tumors. Notably, NK012 eradicated rapid-growing Renca tumors in 6 of 10 mice, whereas it failed to eradicate SKRC-49 tumors. In the pulmonary metastasis treatment model, an enhanced and prolonged distribution of free SN-38 was observed in metastatic lung tissues but not in nonmetastatic lung tissues after NK012 administration. NK012 treatment resulted in a significant decrease in metastatic nodule number and was of benefit to survival. Our study shows the outstanding advantage of polymeric micelle-based drug carriers and suggests that NK012 would be effective in treating disseminated RCCs with irregular vascular architectures. [Cancer Res 2008;68(6):1631–5]

Introduction

Passive targeting of the drug delivery system is suited to combating the pathophysiologic characteristics present in many solid tumors: hypervascularity, irregular vascular architecture, potential for secretion of vascular permeability factors, and the absence of effective lymphatic drainage that prevents efficient clearance of macromolecules. These characteristics, unique to solid tumors, are believed to be the basis of the enhanced permeability and retention (EPR) effect (1). Polymeric micelle-based anticancer drugs have recently been developed (2, 3), and some were put under evaluation for clinical trials (4, 5).

7-Ethyl-10-hydroxy-camptothecin (SN-38), a biological active metabolite of irinotecan hydrochloride (CPT-11), has potent antitumor activity, but has not been used clinically because it is a water-insoluble drug. It has been recently shown that novel SN38-incorporated polymeric micelles, NK012, have the potential to allow effective sustained release of SN-38 inside a tumor and possess potent antitumor activities especially in a vascular endothelial growth factor (VEGF)–secreting hypervascular tumor (6), because the supramolecular structures of NK012 which enable SN-38 to accumulate in the target tissue are based on the EPR effect (1).

Renal cell carcinoma (RCC) is a typical hypervascular tumor with an irregular vascular architecture. We therefore conducted an investigation to determine whether NK012 would be effective in treating RCC by using established RCC tumor models with pulmonary metastasis.

Materials and Methods

Drugs and cells. CPT-11 was purchased from Yakult Honsha Co., Ltd. SN-38 and NK012 was prepared and supplied by Nippon Kayaku Co., Ltd. (6). Five human RCC lines (SKRC-49, Caki-1, 769P, 786O, and KU19-20) and murine Renca cells were maintained in DMEM or MEM supplemented with 2 mmol/L glutamine, 1% nonessential amino acids, 100 units/mL streptomycin and penicillin, and 10% FCS.

***In vitro* growth inhibition assay.** The growth inhibitory effects of NK012, SN-38, and CPT-11 were examined with a 3-(4, 5-dimethylthiazol-2-yl)-2, 5-diphenyltetrazolium bromide (MTT) assay, as described previously (6).

***In vivo* growth inhibition assay.** The animal experimental protocols were approved by the Committee for Ethics of Animal Experimentation, and the experiments were conducted in accordance with the Guidelines for Animal Experiments in the National Cancer Center. Athymic nude mice (3–4 wk old) were maintained in a laminar air flow cabinet under aseptic conditions. 10^7 RCC cells were s.c. injected into the backs of the mice. NK012 at doses of 10 mg/kg/d or 20 mg/kg/d and CPT-11 at doses of 15 mg/kg/d or 30 mg/kg/d were given i.v. on days 0 (when tumors were allowed to grow until they became massive in size, around 1.5 cm), 4, and 8. Tumor volume was determined by direct measurement with calipers and calculated as $\pi/6 \times (\text{large diameter}) \times (\text{small diameter})^2$.

Assessment of treatment effects of NK012 on murine pulmonary metastasis model. A total of 1×10^5 Renca cells were inoculated into male BALB/c mice via the tail vein. The mice were randomly divided into three groups of 10. NK012 at dose of 20 mg/kg/d and CPT-11 at dose of 30 mg/kg/d were given i.v. on days 0 (7 d after inoculation), 4, and 8. After that, the mice were sacrificed, their lungs were stained intratracheally with 15% India black ink solution, and the number of metastatic nodules in each mouse was counted. To determine the effect of NK012 on survival, an identical experiment to the one described above was done. After treatment, mice were maintained until each animal showed signs of morbidity (i.e., over 10% weight loss compared with untreated controls), at which point they were sacrificed. Kaplan-Meier analysis was done to determine the effect on time to morbidity, and statistical differences were ranked according to a Mantel-Cox log-rank test using the StatView 5.0 software package.

Histologic and immunohistochemical analysis. Histologic sections were taken from Renca tumor tissues. After extirpation, tissues were fixed with 3.9% formalin in PBS (pH 7.4), and the subsequent preparations and H&E staining were performed by Tokyo Histopathological Laboratory Co.,

Requests for reprints: Yasuhiro Matsumura, Investigative Treatment Division, Research Center for Innovative Oncology, National Cancer Center Hospital East, 6-5-1 Kashiwanoha, Kashiwa City, Chiba 277-8577, Japan. Phone: 81-4-7134-6857; Fax: 81-4-7134-6857; E-mail: yhmatsum@east.ncc.go.jp.

doi:10.1158/0008-5472.CAN-07-6532

Table 1. *In vitro* growth inhibitory activity of SN-38, NK012, and CPT-11 in RCC lines (MTT assay)

Cell line	IC_{50} (μmol/L)		
	SN-38	NK012*	CPT-11
SKRC-49	0.0064 ± 0.005	0.011 ± 0.008	4.14 ± 0.45
Caki-1	0.0062 ± 0.009	0.032 ± 0.006	8.45 ± 0.85
769P	0.015 ± 0.007	0.085 ± 0.014	34.54 ± 3.76
786O	0.031 ± 0.007	0.12 ± 0.012	28.14 ± 1.21
KU19-20	0.10 ± 0.006	0.34 ± 0.014	32.65 ± 1.25
Renca	0045 ± 0.005	0.0096 ± 0.008	2.26 ± 0.05

*The dose of NK012 is expressed as a dose equivalent to SN-38.

Ltd. Monoclonal anti-CD34 antibody (HyCult Biotechnology) was used to detect the tumor blood vessels. CD34-positive neovessels were counted in 10 high-power fields (×400) by two independent investigators who operated in a blinded fashion.

Assay for free (polymer-unbound) SN-38 in lung tissues. The Renca pulmonary metastasis model described above was used for the analysis of the biodistribution of NK012 and CPT-11. Ten days after Renca inoculation, NK012 (20 mg/kg) or CPT-11 (30 mg/kg) was given i.v. to the mice. The mice were sacrificed at 0, 24, 48, and 72 h after administration, and lung samples were taken and stored at −80°C until analysis. We prepared control mice without Renca inoculation as the nonmetastatic model; NK012 was administrated as well, and lung samples were stored. Samples were then homogenized on ice using a Digital homogenizer (Iuchi) and suspended in the mixture of 100 mmol/L glycine-HCl buffer (pH 3)/methanol (1:1, v/v) at a concentration of 5% w/w. Proteins were precipitated with an ice-cold mixture of 1 mmol/L H_3PO_4/MeOH/H_2O (1:1:4, v/v/v) containing camptothecin as an I.S. The sample was vortexed for 10 s and filtered through a MultiScreen Solvinert (Millipore Corporation), and the concentration of free SN-38 in the aliquots of the homogenates (100 μL) was determined using the high-performance liquid chromatography method (6).

Statistical analysis. Data were expressed as mean ± SD. Significance of differences was calculated using the unpaired *t* test with repeated measures of StatView 5.0. $P < 0.05$ was regarded as statistically significant.

Results and Discussion

We first evaluated *in vitro* cellular sensitivity of RCC lines to SN-38, NK012, and CPT-11. The IC_{50} values of each agent for RCC lines are shown in Table 1. NK012 exhibited higher cytotoxic effect against each cell line compared with CPT-11 (96-fold to 406-fold sensitive).

It is essential to elucidate the correlation between the effectiveness of micellar drugs and tumor hypervascularity and hyperpermeability. Gross evaluation of those RCC tumors s.c. injected into the backs of mice revealed that Renca tumors were more reddish and grew faster than SKRC-49 tumors, and immunohistochemical examination showed that Renca tumors contained much more CD34-positive neovessels than SKRC-49 tumors (Fig. 1).

We allowed the tumors to grow until they became massive, around 1.5 cm, and then initiated treatment. A striking decrease in Renca tumor volume was observed on day 15 in mice treated with NK012 at 20 mg/kg/d compared with the untreated control (Fig. 2*A*). Renca bulky masses completely disappeared on day 21 in 6 of 10 mice treated with NK012 at 20 mg/kg/d. On the other hand, Renca tumors in mice treated with CPT-11 at 30 mg/kg/d were not eradicated and rapidly regrew after a partial response at day 15. An approximate 10% body weight loss occurred in mice treated with NK012 20 mg/kg, compared with the untreated controls, but there was no significant difference in comparison with tumor-free mice treated with NK012, suggesting that the decrease in body weight was likely to be due to tumor shrinkage rather than toxic effects. We next compared the antitumor activities of the NK012 and CPT-11 treatment in SKRC-49 and Renca tumors. The SKRC-49 tumor volume in mice treated with NK012 at 20 mg/kg/d on day 21 was over 70% smaller than in the untreated controls on day 21 and −50% smaller than in mice on day 0 (Fig. 2*B*). However, the SKRC-49 tumors were not eradicated in mice treated with NK012. Considering that equivalent *in vitro* growth inhibitory effects by NK012 were observed for SKRC-49 and Renca cells (Table 1), our results suggest that the antitumor activity of NK012 *in vivo* might be affected by tumor environment factors, such as tumor vascularity.

We next examined the distribution of free SN-38 in the metastatic or nonmetastatic (no inoculation of Renca cells) lung tissues after administration of NK012 or CPT-11. In the case of NK012 administration in mice with lung metastasis, free SN-38 was detectable at the concentration of >100 ng/g in metastatic lung tissues with a typical microvascular architecture (Fig. 3*A*) even at 72 hours after administration, whereas the concentrations of free SN-38 in nonmetastatic lung tissues after NK012 administration were much lower than those in metastatic lung tissues after treatment with NK012 (significant at 24, 48, and 72 hours; $P < 0.05$;

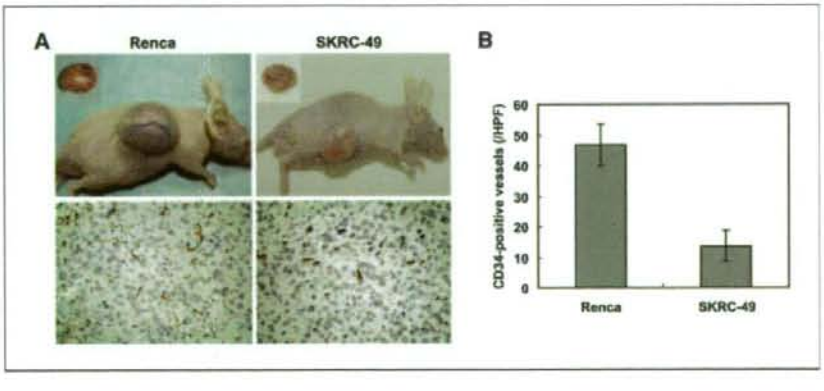

Figure 1. Comparison of tumor angiogeneses of Renca and SKRC-49 in athymic nude mice. *A*, representative photographs of massive tumors developed from Renca and SKRC-49 at 28 d after s.c. injection (inoculation). Immunohistochemical (CD34, ×400) examinations for each tumor are shown. *B*, tumor neovascularization in each tumor was quantified by counting CD34-positive neovessels. *Bars*, SD. Experiments were repeated twice with similar results.

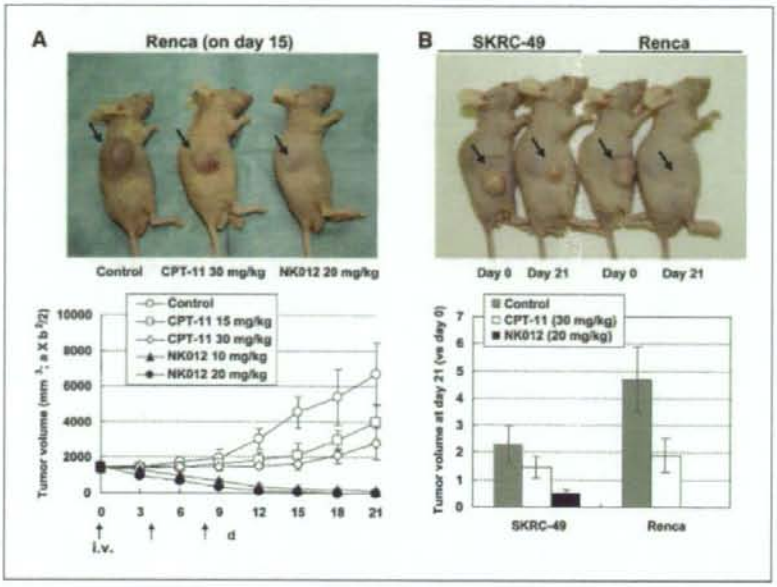

Figure 2. Growth-inhibitory effect of NK012 and CPT-11 on bulky RCC tumors. I.v. administration of NK012 or CPT-11 was started when the mean tumor volumes of groups reached a massive 1,500 mm^3. The mice were divided into test groups as indicated. *A*, representative of each group at day 15 in the Renca allograft model. *Arrows*, Renca allografts (*top*). Time profile of tumor volume in mice treated with NK012 or CPT-11 at indicated doses (*bottom*). Each group consisted of 10 mice. *Bars*, SD. *B*, the comparison of antitumor activities of CPT-11 and NK012 in SKRC-49 xenografts and Renca allografts. Representative of mice treated with NK012 at day 0 and day 21. Experiments were repeated twice with similar results. The mice at day 0 in the photograph belong to the group in the second experiment which started just at day 21 of the first experiment. *Arrows*, tumor grafts. The relative tumor volume values at day 21 to those at day 0 in each group set to 1 (*bottom*). Each group consisted of 10 mice.

Fig. 3*B*). On the other hand, the concentrations of free SN-38 after administration of CPT-11 were almost negligible in metastatic lung tissues at all time points (data not shown). These results strongly suggest that SN-38 could be selectively released from NK012 and maintained in metastatic Renca tumor tissues.

Deviating from the ordinary experimental pulmonary metastasis prevention model, we initiated treatment 7 days after inoculation (day 0) when multiple lung nodules derived from Renca were observed in all mice in our preliminary study (Fig. 4*A*). On day 21, there was no significant difference between the mean number of metastatic nodules in the control group (287 ± 56 nodules, $n = 10$) and in the group receiving CPT-11 treatment (236 ± 59 nodules, $n = 10$). Significant treatment effects were found, however, in the group receiving NK012 treatment (32 ± 18 nodules, $n = 10$) on day 21 compared with the control group on day 21 ($P < 0.0001$). Notably, a dramatic decrease in metastatic nodule number was observed in the NK012 treatment group on day 21 compared with the control group on day 0 (126 ± 23 nodules, $n = 10$, $P < 0.001$; Fig. 4*A*). Kaplan-Meier analysis showed that a significant survival benefit was obtained in the NK012 treatment group compared with

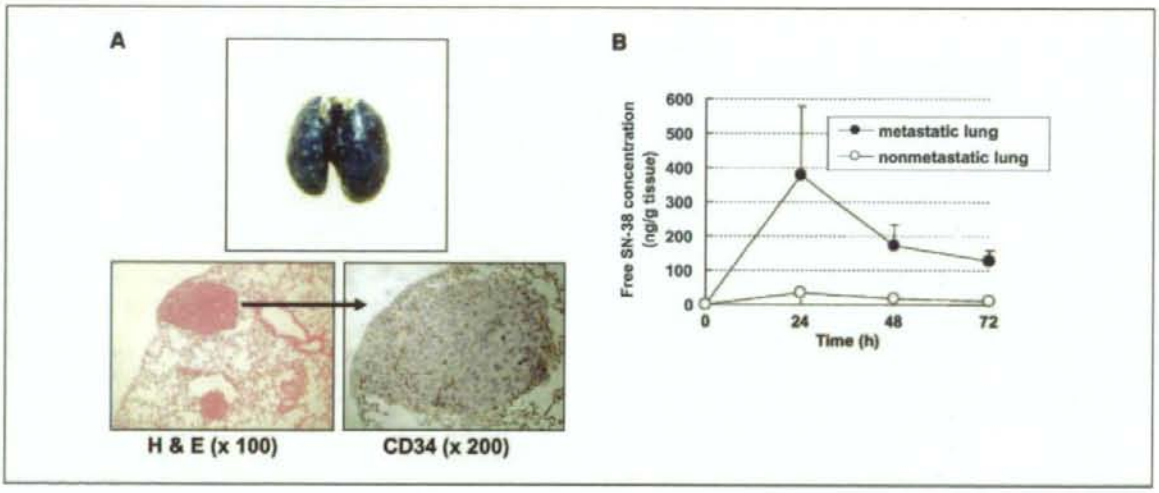

Figure 3. Pulmonary metastasis of Renca cells and lung tissue distribution of free SN-38 after administration of NK012 and CPT-11. *A*, gross appearances of pulmonary metastasis observed 7 d after Renca inoculation (*top*). Multiple metastatic nodules and neovascularization in metastatic lung tumor lesion (*bottom*). *B*, time profile of free SN-38 concentration in metastatic or nonmetastatic lung tissues in mice treated with NK012 (20 mg/kg/d). *Bars*, SD. Experiments were performed in tetraplicate.

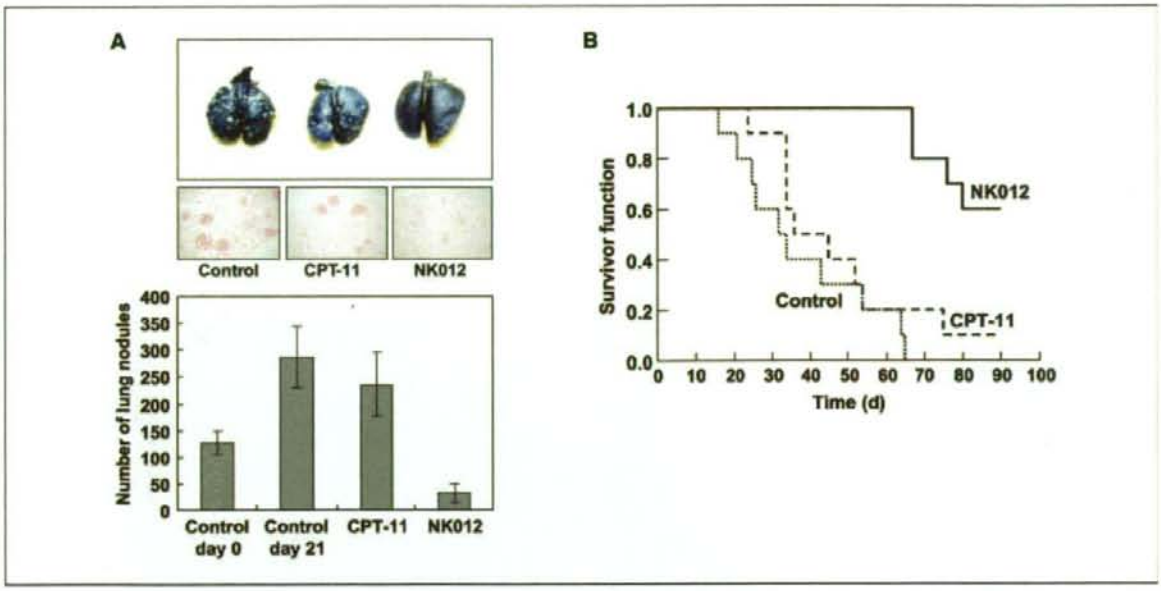

Figure 4. Treatment effect of NK012 on established pulmonary metastasis and survival. NK012 (20 mg/kg/d) and CPT-11 (30 mg/kg/d) were given i.v. to mice with established pulmonary metastasis on days 0 (7 d after Renca inoculation), 4, and 8. *A*, gross and histologic appearances of pulmonary metastases at day 21 (*top*). The metastatic nodules in each mouse were counted. Each group consisted of five mice. *B*, mice were maintained for 90 d after each treatment and survival was assessed by a Kaplan-Meier analysis. Each group consisted of five mice. Experiments were repeated twice with similar results.

the control group ($P < 0.001$), but no significant survival benefit was obtained in CPT-11 treatment group ($P = 0.239$; Fig. 4*B*). Although no severe toxic effects were observed in any mouse treated with NK012, 3 of 10 mice treated with NK012 were sacrificed during the observation period according to the 'Guidelines for Animal Experiments because their body weights had become 10% lower than those of the other mice. However, the sacrificed mice were a little bit smaller than others when they started treatment, and they showed no disseminated lung metastasis (data not shown).

Our results presented here strongly support recent findings reported by us that the macromolecular drug distribution throughout the tumor site was enhanced by the hypervascularity and hyperpermeability, and subsequently higher antitumor activity was achieved (6). We assume that conventional low molecular size anticancer agents almost disappear from the bloodstream without being subjected to the EPR effect before they can reach the target organs (solid tumor). The clinical importance of angiogenesis in human tumors has been shown in several reports indicating a positive relationship between the blood vessel density in the tumor mass and poor prognosis with chemoresistance in patients with various cancers (7–9). Furthermore, recent reports showing that anticancer agents were less active against VEGF-overexpressing tumors (10, 11) may support the idea that low-molecular drugs are not so effective in the treatment of solid tumors which are rich in blood vessels.

Our study thus far has several limitations about clarifying whether extensive angiogenesis in the tumor is an essential determinant for the susceptibility to NK012. In our ongoing study, we found that NK012 also has a striking antitumor activity against some hypovascular tumor models of human pancreatic cancer xenografts.[5] It also remains unclear whether NK012 possesses strong antitumor activity in other metastatic sites besides the lung. It is known that the EPR effect is affected by various permeability factors, such as bradykinin (12), nitric oxide (13), and various cytokines independent of VEGF and hypervascularity (14). Among solid tumors with rapid progression potential, irregularity occurs not only in blood flow and vascular density, but also in the vascular network and anatomic architecture (15, 16), suggesting that EPR effect may be predominantly promoted in rapid-progressive tumor phenotypes and influenced by organ-specific tumor microenvironment. Hoffman and coworkers (17, 18) have developed a technique of surgical orthotopic implantation (SOI) with more clinical features of systemic and aggressive metastases than our conventional animal models. Further preclinical studies using such models as SOI might clarify cancer phenotypes and metastatic organs to which we can apply NK012 more precisely.

The results of chemotherapy in RCCs have been disappointing, as indicated by the low response proportions. However, clinical trials using gemcitabine-containing regimens have been encouraging, with major responses occurring in 5% to 17% of patients (19, 20), suggesting the possibility that chemotherapy is promising as a modality for RCC therapy if anticancer agents can be selectively delivered, released, and maintained around tumor tissues. Our current report highlights the advantages of polymeric micelle-based drug carriers like NK012 as promising modalities for treatment, rather than prevention, of disseminated RCCs with abnormal vascular architecture. The results of our ongoing phase-I

[5] Y. Saito, M. Yasumaga, J. Kuroda, Y. Koga, and Y. Matsumura. Unpublished data.

clinical trial and future phase-II trials of NK012 in patients with advanced solid tumors including RCC might meet or even exceed our expectations.

Acknowledgments

Received 12/10/2007; revised 1/25/2008; accepted 1/31/2008.

Grant support: Grant-in-aid from 3rd Term Comprehensive Control Research for Cancer, Ministry of Health, Labor and Welfare (Y. Matsumura) and Scientific Research on Priority Areas from the Ministry of Education, Culture, Sports, Science and Technology (Y. Matsumura).

The costs of publication of this article were defrayed in part by the payment of page charges. This article must therefore be hereby marked *advertisement* in accordance with 18 U.S.C. Section 1734 solely to indicate this fact.

We thank H. Miyatake and N. Mie for their technical assistance and K. Shiina for her secretarial assistance.

References

1. Matsumura Y, Maeda H. A new concept for macromolecular therapeutics in cancer chemotherapy: mechanism of tumoritropic accumulation of proteins and the antitumor agent smancs. Cancer Res 1986;46:6387–92.
2. Yokoyama M, Miyauchi M, Yamada N, et al. Characterization and anticancer activity of the micelle-forming polymeric anticancer drug adriamycin-conjugated poly(ethylene glycol)-poly(aspartic acid) block copolymer. Cancer Res 1990;50:1693–700.
3. Kataoka K, Harada A, Nagasaki Y. Block copolymer micelles for drug delivery: design, characterization and biological significance. Adv Drug Deliv Rev 2001;47:113–31.
4. Matsumura Y, Hamaguchi T, Ura T, et al. Phase I clinical trial and pharmacokinetic evaluation of NK911, a micelle-encapsulated doxorubicin. Br J Cancer 2004;91:1775–81.
5. Hamaguchi T, Kato K, Yasui H, et al. A phase I and pharmacokinetic study of NK105, a paclitaxel-incorporating micellar nanoparticle formulation. Br J Cancer 2007;97:170–6.
6. Koizumi F, Kitagawa M, Negishi T, et al. Novel SN-38-incorporating polymeric micelles, NK012, eradicate vascular endothelial growth factor-secreting bulky tumors. Cancer Res 2006;66:10048–56.
7. Gasparini G, Harris AL. Clinical importance of the determination of tumor angiogenesis in breast carcinoma: much more than a new prognostic tool. J Clin Oncol 1995;13:765–82.
8. Takahashi Y, Kitadai Y, Bucana CD, Cleary KR, Ellis LM. Expression of vascular endothelial growth factor and its receptor, KDR, correlates with vascularity, metastasis, and proliferation of human colon cancer. Cancer Res 1995;55:3964–8.
9. Williams JK, Carlson GW, Cohen C, Derose PB, Hunter S, Jurkiewicz MJ. Tumor angiogenesis as a prognostic factor in oral cavity tumors. Am J Surg 1994;168:373–80.
10. Natsume T, Watanabe J, Koh Y, et al. Antitumor activity of TZT-1027 (Soblidotin) against vascular endothelial growth factor-secreting human lung cancer *in vivo*. Cancer Sci 2003;94:826–33.
11. Zhang L, Hannay JA, Liu J, et al. Vascular endothelial growth factor overexpression by soft tissue sarcoma cells: implications for tumor growth, metastasis, and chemoresistance. Cancer Res 2006;66:8770–8.
12. Matsumura Y, Maruo K, Kimura M, Yamamoto T, Konno T, Maeda H. Kinin-generating cascade in advanced cancer patients and *in vitro* study. Jpn J Cancer Res 1991;82:732–41.
13. Wu J, Akaike T, Hayashida K, et al. Identification of bradykinin receptors in clinical cancer specimens and murine tumor tissues. Int J Cancer 2002;98:29–35.
14. Maeda H, Fang J, Inutsuka T, Kitamoto Y. Vascular permeability enhancement in solid tumor: various factors, mechanisms involved and its implications. Int Immunopharmacol 2003;3:319–28.
15. Suzuki M, Takahashi T, Sato T. Medial regression and its functional significance in tumor-supplying host arteries. A morphometric study of hepatic arteries in human livers with hepatocellular carcinoma. Cancer 1987;59:444–50.
16. Skinner SA, Tutton PJ, O'Brien PE. Microvascular architecture of experimental colon tumors in the rat. Cancer Res 1990;50:2411–7.
17. An Z, Jiang P, Wang X, Moossa AR, Hoffman RM. Development of a high metastatic orthotopic model of human renal cell carcinoma in nude mice: benefits of fragment implantation compared to cell-suspension injection. Clin Exp Metastasis 1999;17:265–70.
18. Hoffman RM. Orthotopic metastatic mouse models for anticancer drug discovery and evaluation: a bridge to the clinic. Invest New Drugs 1999;17:343–59.
19. Rini BI, Vogelzang NJ, Dumas MC, Wade JL III, Taber DA, Stadler WM. Phase II trial of weekly intravenous gemcitabine with continuous infusion fluorouracil in patients with metastatic renal cell cancer. J Clin Oncol 2000;18:2419–26.
20. Nanus DM, Garino A, Milowsky MI, Larkin M, Dutcher JP. Active chemotherapy for sarcomatoid and rapidly progressing renal cell carcinoma. Cancer 2004;101:1545–51.

Int. J. Cancer: **122,** 2148–2153 (2008)

Synergistic antitumor activity of the novel SN-38-incorporating polymeric micelles, NK012, combined with 5-fluorouracil in a mouse model of colorectal cancer, as compared with that of irinotecan plus 5-fluorouracil

Takako Eguchi Nakajima[1,2], Masahiro Yasunaga[2], Yasuhiko Kano[3], Fumiaki Koizumi[4], Ken Kato[1], Tetsuya Hamaguchi[1], Yasuhide Yamada[1], Kuniaki Shirao[1], Yasuhiro Shimada[1] and Yasuhiro Matsumura[2]*

[1]*Gastrointestinal Oncology Division, National Cancer Center Hospital, Tokyo, Japan*
[2]*Investigative Treatment Division, Research Center for Innovative Oncology, National Cancer Center Hospital East, Kashiwa, Chiba, Japan*
[3]*Hematology Oncology, Tochigi Cancer Center, Tochigi, Japan*
[4]*Shien Lab Medical Oncology Division, National Cancer Center Hospital, Tokyo, Japan*

The authors reported in a previous study that NK012, a 7-ethyl-10-hydroxy-camptothecin (SN-38)-releasing nano-system, exhibited high antitumor activity against human colorectal cancer xenografts. This study was conducted to investigate the advantages of NK012 over irinotecan hydrochloride (CPT-11) administered in combination with 5-fluorouracil (5FU). The cytotoxic effects of NK012 or SN-38 (an active metabolite of CPT-11) administered in combination with 5FU was evaluated *in vitro* in the human colorectal cancer cell line HT-29 by the combination index method. The effects of the same drug combinations was also evaluated *in vivo* using mice bearing HT-29 and HCT-116 cells. All the drugs were administered i.v. 3 times a week; NK012 (10 mg/kg) or CPT11 (50 mg/kg) was given 24 hr before 5FU (50 mg/kg). Cell cycle analysis in the HT-29 tumors administered NK012 or CPT-11 *in vivo* was performed by flow cytometry. NK012 exerted more synergistic activity with 5FU compared to SN-38. The therapeutic effect of NK012/5FU was significantly superior to that of CPT-11/5FU against HT-29 tumors ($p = 0.0004$), whereas no significant difference in the antitumor effect against HCT-116 tumors was observed between the 2-drug combinations ($p = 0.2230$). Cell-cycle analysis showed that both NK012 and CPT-11 tend to cause accumulation of cells in the S phase, although this effect was more pronounced and maintained for a more prolonged period with NK012 than with CPT-11. Optimal therapeutic synergy was observed between NK012 and 5FU, therefore, this regimen is considered to hold promise of clinical benefit, especially for patients with colorectal cancer.

Key words: NK012; SN-38; 5-fluorouracil; drug delivery system; colorectal cancer

The 5-year survival rates of colorectal cancer (CRC) have improved remarkably over the last 10 years, accounted for in large part by the extensively investigated agents after 5-fluorouracil (5FU). Irinoetcan hydrochloride (CPT-11), a water-soluble, semi-synthetic derivative of camptothecin, is one such agent that has been shown to be highly effective, and currently represents a key-drug in first- and second-line treatment regimens for CRC. CPT-11 monotherapy, however, has not been shown to yield superior efficacy, including in terms of the median survival time, to bolus 5FU/leucovorin (LV) alone.[1] In 2 Phase III trials, the addition of CPT-11 to bolus or infusional 5FU/LV regimens clearly yielded greater efficacy than administration of 5FU/LV alone, with a doubling of the tumor response rate and prolongation of the median survival time by 2–3 months.[1,2]

CPT-11 is converted to 7-ethyl-10-hydroxy-camptothecin (SN-38), a biologically active and water-insoluble metabolite of CPT-11, by carboxylesterases in the liver and the tumor. SN-38 has been demonstrated to exhibit up to a 1,000-fold more potent cytotoxic activity than CPT-11 against various cancer cells *in vitro*.[3] The metabolic conversion rate is, however, very low, with only <10% of the original volume of CPT-11 being metabolized to SN-38[4,5]; conversion of CPT-11 to SN-38 also depends on genetic interindividual variability of the activity of carboxylesterases.[6] Direct use of SN-38 itself for clinical cancer treatment must be shown to be identical in terms of both efficacy and toxicity.

Some drugs incorporated in drug delivery systems (DDS), such as Abraxane and Doxil, are already in clinical use.[7,8] The clinical benefits of DDS are based on their EPR effect.[9] The EPR effect is based on the pathophysiological characteristics of solid tumor tissues: hypervascularity, incomplete vascular architecture, secretion of vascular permeability factors stimulating extravasation within cancer tissue, and absence of effective lymphatic drainage from the tumors that impedes the efficient clearance of macromolecules accumulated in solid tumor tissues. Several types of DDS can be used for incorporation of a drug. A liposome-based formulation of SN-38 (LE-SN38) has been developed, and a clinical trial to assess its efficacy is now under way.[10,11]

Recently, we demonstrated that NK012, novel SN-38-incorporating polymeric micelles, exerted superior antitumor activity and less toxicity than CPT-11.[12] NK012 is characterized by a smaller size of the particles than LE-SN38; the mean particle diameter of NK012 is 20 nm. NK012 can release SN-38 under neutral conditions even in the absence of a hydrolytic enzyme, because the bond between SN-38 and the block copolymer is a phenol ester bond, which is stable under acidic conditions and labile under mild alkaline conditions. The release rate of SN-38 from NK012 under physiological conditions is quite high; more than 70% of SN-38 is released within 48 hr. We speculated that the use of NK012, in place of CPT-11, in combination with 5FU may yield superior results in the treatment of CRC. In the present study, we evaluated the antitumor activity of NK012 administered in combination with 5FU as compared to that of CPT-11 administered in combination with 5FU against CRC in an experimental model.

Material and methods

Cells and animals

The human colorectal cancer cell lines used, namely, HT-29 and HCT-116, were purchased from the American Type Culture Collection (Rockville, MD). The HT-29 cells and HCT-116 cells were maintained in RPMI 1640 supplemented with 10% fetal bovine serum (Cell Culture Technologies, Gaggenau-Hoerden, Germany), penicillin, streptomycin, and amphotericin B (100 units/mL, 100 μg/mL, and 25 μg/mL, respectively; Sigma, St. Louis, MO) in a humidified atmosphere containing 5% CO_2 at 37°C.

BALB/c *nu/nu* mice were purchased from SLC Japan (Shizuoka, Japan). Six-week-old mice were subcutaneously (s.c.)

***Correspondence to:** Investigative Treatment Division, Research Center for Innovative Oncology, National Cancer Center Hospital East, 6-5-1 Kashiwanoha, Kashiwa, Chiba 277-8577, Japan. Fax: +81-4-7134-6866. E-mail: yhmatsum@east.ncc.go.jp
Received 2 September 2007; Accepted after revision 20 November 2007
DOI 10.1002/ijc.23381
Published online 14 January 2008 in Wiley InterScience (www.interscience.wiley.com).

inoculated with 1×10^6 cells of HT-29 or HCT-116 cell line in the flank region. The length (a) and width (b) of the tumor masses were measured twice a week, and the tumor volume (TV) was calculated as follows: $TV = (a \times b^2)/2$. All animal procedures were performed in compliance with the Guidelines for the Care and Use of Experimental Animals established by the Committee for Animal Experimentation of the National Cancer Center; these guidelines meet the ethical standards required by law and also comply with the guidelines for the use of experimental animals in Japan.

Drugs

The SN-38-incorporating polymeric micelles, NK012, and SN-38 were prepared by Nippon Kayaku (Tokyo, Japan).[12] CPT-11 was purchased from Yakult Honsha (Tokyo, Japan). 5FU was purchased from Kyowa Hakko (Tokyo, Japan).

Cell growth inhibition assay

HT-29 cells were seeded in 96-well plates at a density of 2,000 cells/well in a final volume of 90 μL. Twenty-four hours after seeding, a graded concentration of NK012 or SN-38 was added concurrently with 5FU to the culture medium of the HT-29 cells in a final volume of 100 μL for drug interaction studies. The culture was maintained in the CO_2 incubator for an additional 72 hr. Then, cell growth inhibition was measured by the tetrazolium salt-based proliferation assay (WST assay; Wako Chemicals, Osaka, Japan). WST-1 labeling solution (10 μL) was added to each well and the plates were incubated at 37°C for 3 hr. The absorbance of the formazan product formed was detected at 450 nm in a 96-well spectrophotometric plate reader. Cell viability was measured and compared to that of the control cells. Each experiment was carried out in triplicate and was repeated at least 3 times. Data were averaged and normalized against the nontreated controls to generate dose-response curves.

Drug interaction analysis

The nature of interaction between NK012 or SN-38 and 5FU against HT-29 cells was evaluated by median-effect plot analyses and the combination index (CI) method of Chou and Talalay.[13] Data analysis was performed using the Calcusyn software (Biosoft, NY, USA). NK012 or SN-38 was combined with 5FU at a fixed ratio that spanned the individual IC_{50} values of each drug. The IC_{50} values were determined on the basis of the dose-response curves using the WST assay. For any given drug combination, the CI is known to represent the degree of synergy, additivity or antagonism. It is expressed in terms of fraction-affected (Fa) values, which represents the percentage of cells killed or inhibited by the drug. Isobologram equations and Fa/CI plots were constructed by computer analysis of the data generated from the median effect analysis. Each experiment was performed in triplicate with 6 gradations and was repeated at least 3 times. The resultant dose-response curves were averaged, to create a single composite dose-response curve for each combination.

In vivo analysis of the effects of NK012 combined with 5FU as compared to those of CPT-11 combined with 5FU

When the mean tumor volumes reached ~93 mm^3, the mice were randomly divided into test groups consisting of 5 mice per group (Day 0). The drugs were administered i.v. *via* the tail vein of the mice. In the groups administered NK012 or 5FU as single agents, the drug was administered on Days 0, 7 and 14. In the combined treatment groups, NK012 or CPT-11 was administered 24 hr before 5FU on Days 0, 7 and 14, according to the previously reported combination schedule for CPT-11 and 5FU.[14] Complete response (CR) was defined as tumor not detectable by palpation at 90 days after the start of treatment, at which time-point the mice were sacrificed. Tumor volume and body weight were measured twice a week. As a general rule, animals in which the tumor volume exceeded 2,000 mm^3 were also sacrificed.

Experiment 1. Evaluation of the effects of NK012 combined with 5FU and determination of the maximum tolerated dose (MTD) of NK012/5FU. By comparing the data between NK012 administered as a single agent and NK012/5FU, we evaluated the effects of the combined regimen against the s.c HT-29 tumors. A preliminary experiment showed that combined administration of NK012 15 mg/kg + 5FU 50 mg/kg every 6 days caused drug-related lethality (data not shown). To determine the MTD, therefore, we set the dosing schedule of the combined regimen at 5 or 10 mg/kg of NK012 + 50 mg/kg of 5FU three times a week.

Experiment 2. Comparison of the antitumor effect of NK012/5FU and CPT-11/5FU. Based on a comparison of the data between NK012/5FU and CPT-11/5FU against the s.c. HT-29 and HCT-116 tumors, we investigated the feasibility of the clinical application of NK012/5FU for the treatment of CRC. CPT-11/5FU was administered three times a week at the respective MTDs of the 2 drugs as previously reported, that is, CPT11 at 50 mg/kg and 5FU at 50 mg/kg, respectively.[14] NK012/5FU was administered once three times a week at the respective MTDs of the 2 drugs determined from Experiment 1.

Cell cycle analysis

Samples from the HT-29 tumors that had grown to 80–100 mm^3 were removed from the mice at 6, 24, 48, 72 and 96 hr after the administration of NK012 alone at 10 mg/kg or CPT-11 alone at 50 mg/kg. The samples were excised, minced in PBS and fixed in 70% ethanol at −20°C for 48 hr. They were then digested with 0.04% pepsin (Sigma chemical Co., St Lous, MO) in 0.1 N HCL for 60 min at 37°C in a shaking bath to prepare single-nuclei suspensions. The nuclei were then centrifuged, washed twice with PBS and stained with 40 μg/mL of propidium iodide (Molecular Probes, OR) in the presence of 100 μg/mL RNase in 1 mL PBS for 30 min at 37°C. The stained nuclei were analyzed with B-D FACSCalibur (BD Biosciences, San Jose, CA), and the cell cycle distribution was analyzed using the Modfit program (Verity Software House Topsham, ME).

Statistical analyses

Data were expressed as mean ± SD. Data were analysed with Student's t test when the groups showed equal variances (F test), or Welch's test when they showed unequal variances (F test). $p < 0.05$ was regarded as statistically significant. All statistical tests were 2-sided.

Results

Antiproliferative effects of NK012 or SN-38 administered in combination with 5FU

Figure 1*a* shows the dose-response curves for NK012 alone, 5FU alone and a combination of the two. The IC_{50} levels of NK012 and 5FU against the HT-29 cells were 39 nM and 1 μM, respectively, and the IC_{50} level of SN-38 was 14 nM (data not shown). Based on these data, the molar ratio of NK012 or SN-38:5FU of 1:1,000 was used for the drug combination studies.

Figures 1*b* and 1*c* show the median-effect and the combination index plots. Combination indices (CIs) of <1.0 are indicative of synergistic interactions between 2 agents; additive interactions are indicated by CIs of 1.0, and antagonism by CIs of >1.0. Figure 1*c* shows the combination index for NK012 and 5FU, when 2 drugs are supposed to be mutually exclusive. Marked synergism was observed between Fa 0.2 and 0.6. Theoretically, the CI method is the most reliable around an Fa of 0.5, suggesting synergistic effects of the combination of NK012 and 5FU. This synergistic effect was more evident than that of SN-38/5FU (Fig. 1*d*).

In vivo *effect of combined NK012 and 5FU*

Experiment 1. Dose optimization and effect of combined NK012 and 5FU against HT-29 tumors. Comparison of the relative tumor volumes on Day 40 revealed significant differences between

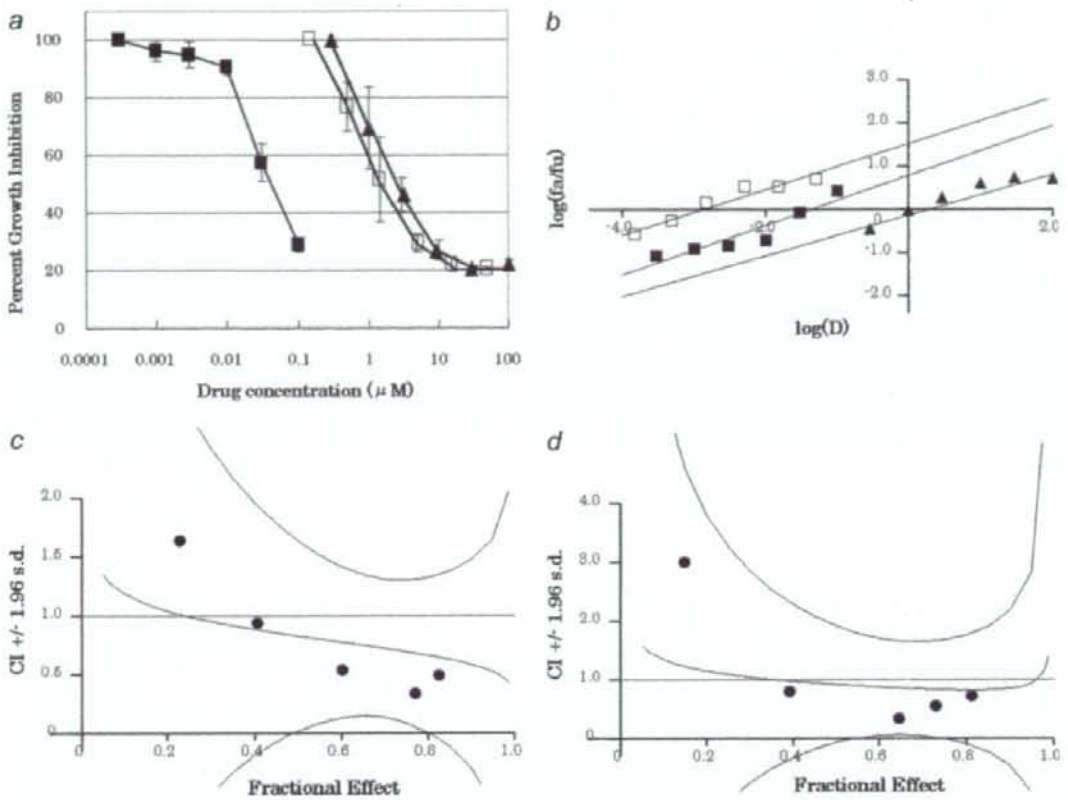

FIGURE 1 – Interaction of NK012 and 5FU *in vitro*. (*a*) Dose-response curves for NK012 alone (■), 5FU alone (▲) and their combination (□) against HT-29 cells. HT-29 cells were seeded at 2,000 cells/well. Twenty-four hours after seeding, a graded concentration of NK012 or 5FU was added to the culture medium of the HT-29 cells. Cell growth inhibition was measured by WST assay after 72 hr of treatment. Cell viability was measured and compared with that of the control cells. Each experiment was carried out independently and repeated at least 3 times. Points, mean of tripricates; bars, SD. (*b*) Median effect plot for the interaction of NK012 and 5FU. (*c*, *d*) Combination index for the interaction as a function of the level of effect (fraction effect = 0.5 is the IC_{50}). The straight line across the CI value of 1.0 indicates additive effect and CIs above and below indicate antagonism and synergism, respectively. The molar ratio of NK012/5FU (*c*) or SN-38/5FU (*d*) at 1:1,000 was tested by CI analysis. Black circles represent the CIs of the actual data points, solid lines represent the computer-derived CIs at effect levels ranging from 10 to 100% inhibition of cell growth, and the dotted lines represent the 95% confidence intervals.

those in the mice administered NK012 alone and those administered NK012/5FU at 5 mg/kg of NK012 ($p = 0.018$) (Fig. 2*a*). Although there was no statistically significant difference in the relative tumor volume measured on Day 54 between the mice administered NK012 alone and NK012/5FU at 10 mg/kg of NK012 ($p = 0.3050$), a trend of superior antitumor effect was demonstrated in the group treated with NK012/5FU at 10 mg/kg of NK012 (Fig. 2*a*). The CR rates were 20, 40 and 60% for 5 mg/kg NK012 + 50 mg/kg 5FU, 10 mg/kg NK012 alone and 10 mg/kg NK012 + 50 mg/kg 5FU, respectively. The schedule of 10 mg/kg NK012 + 50 mg/kg 5FU resulted in no remarkable toxicity in terms of body weight changes, and these doses were determined as representing the MTDs (Fig. 2*b*).

Experiment 2. Comparison of the antitumor effect of combined NK012/5FU and CPT-11/5FU against HT-29 and HCT-116 tumors. The therapeutic effect of NK012/5FU on Day 60 was significantly superior to that of CPT-11/5FU against the HT-29 tumors ($p = 0.0004$) (Fig. 3*a*). A more potent antitumor effect, namely, a 100% CR rate, was obtained in the NK012/5FU group as compared to the 0% CR rate in the CPT-11/5FU group. Although no statistically significant difference in the relative tumor volume on Day 61 was demonstrated between the NK012/5FU and CPT-11/5FU in the case of the HCT-116 tumors ($p = 0.2230$), a trend of superior antitumor effect against these tumors was observed in the NK012/5FU treatment group (Fig. 3*b*). The CR rates for the case of the HCT-116 tumors were 0% in both NK012/5FU and CPT-11/5FU groups.

Specificity of cell cycle perturbation

We studied the differences in the effects between NK012 10 mg/kg and CPT-11 50 mg/kg on the cell cycle (Fig. 4*a*). The data indicated that both NK012 and CPT-11 tended to cause accumulation of cells in the S phase, although the effect of NK012 was stronger and maintained for a more prolonged period than that of CPT-11; the maximal percentage of S-phase cells in the total cell population in the tumors was 34% at 24 hr after the administration of CPT-11, whereas it was 39% at 48 hr after the administration of NK012 (Figs. 4*b*, and 4*c*).

Discussion

Our primary endpoint was to clarify the advantages of NK012 over CPT-11 administered in combination with 5FU. We demonstrated that combined NK012 and 5FU chemotherapy exerts more

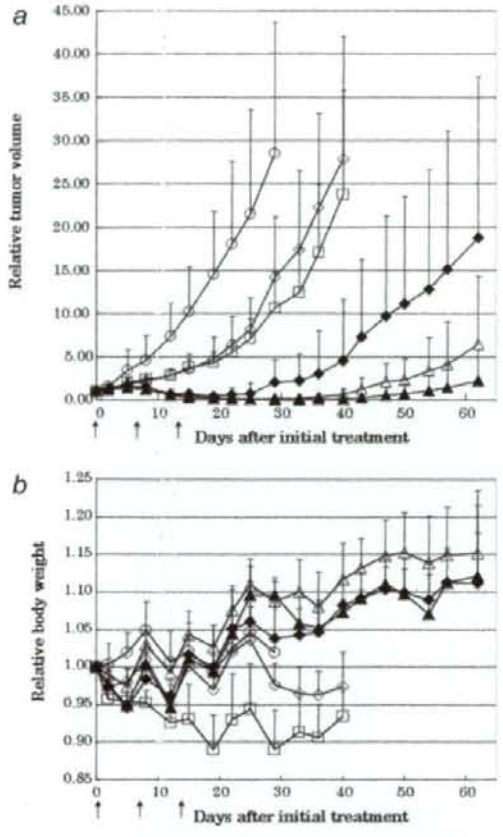

FIGURE 2 – Effect of NK012 alone or NK012 in combination with 5FU against HT-29 tumor-bearing mice. Points, mean; bars, SD. (*a*) Antitumor effect of each regimen on Days 0, 7 and 14. (○) control, (□) 5FU 50 mg/kg alone, (◇) NK012 5 mg/kg alone, (◆) NK012 5 mg/kg 24 hr before 5FU 50 mg/kg, (△) NK012 10 mg/kg alone, (▲) NK012 10 mg/kg 24 hr before 5FU 50 mg/kg. (*b*) Changes in the relative body weight. Data were derived from the same mice as those used in the present study.

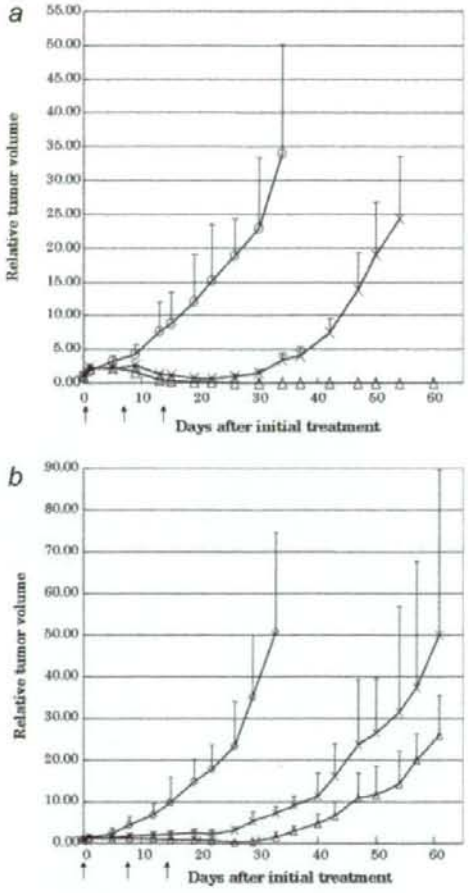

FIGURE 3 – Effect of NK012/5FU as compared with that of CPT11/5FU against HT-29 (*a*) or HCT-116 (*b*) tumor-bearing mice. Antitumor effect of each schedule on Days 0, 7 and 14. (○) control, (×) CPT-11 50 mg/kg 24 hr before 5FU 50 mg/kg, (△) NK012 10 mg/kg 24 hr before 5FU 50 mg/kg. Points, mean; bars, SD.

synergistic activity *in vitro* and significantly greater antitumor activity against human CRC xenografts as compared to CPT-11/5FU. The combination of NK012 and 5FU is considered to hold promise of clinical benefit for patients with CRC.

CPT-11, a topoisomerase-I inhibitor, and 5FU, a thymidilate synthase inhibitor, have been demonstrated to be effective agents for the treatment of CRC. A combination of these 2 drugs has also been demonstrated to be clearly more effective than either CPT-11 or 5FU/LV administered alone *in vivo* and in clinical settings.[1,2,14] Administration of 5FU by infusion with CPT-11 was shown to be associated with reduced toxicity and an apparent improvement in survival as compared to that of administration of the drug by bolus injection with CPT-11.[1,2] This synergistic enhancement may result from the mechanism of action of the 2 drugs; CPT-11 has been reported to cause accumulation of cells in the S phase, and 5FU infusion is known to cause DNA damage specifically in cells of the S phase.[14] On the basis of this background, our results suggesting the more pronounced and more prolonged accumulation of the tumor cells in the S phase caused by NK012 as compared with that by CPT-11 may explain the more effective synergy of the former administered with 5FU infusion. This may be attributable to accumulation of NK012 due to the enhanced permeability and retention (EPR) effect.[9] It is also speculated that NK012 allows sustained release of free SN-38, which may move more freely in the tumor interstitium.[15] Otherwise NK012 itself could internalize into cells to localize in several cytoplasmic organelles as reported by Savic *et al.*[16] These characteristics of NK012 may be responsible for its more potent antitumor activity observed in this study, because CPT-11 has been reported to show time-dependent growth-inhibitory activity against the tumor cells.[17]

The major dose-limiting toxicities of CPT-11 are diarrhea and neutropenia. SN-38, the active metabolite of CPT-11, may cause CPT-11-related diarrhea as a result of mitotic -inhibitory activity.[18] Because it undergoes significant biliary excretion, SN-38 may have a potentially long residence time in the gastrointestinal tract that may be associated with prolonged diarrhea.[19,20] In our previous report, we evaluated the tissue distribution of SN-38 after administration of an equimolar amount of NK012 (20 mg/kg) and CPT-11 (30 mg/kg), and found no difference in the level of SN-38 accumulation in the small intestine.[12] A significant antitumor effect of NK012 with a lower incidence of diarrhea was also dem-

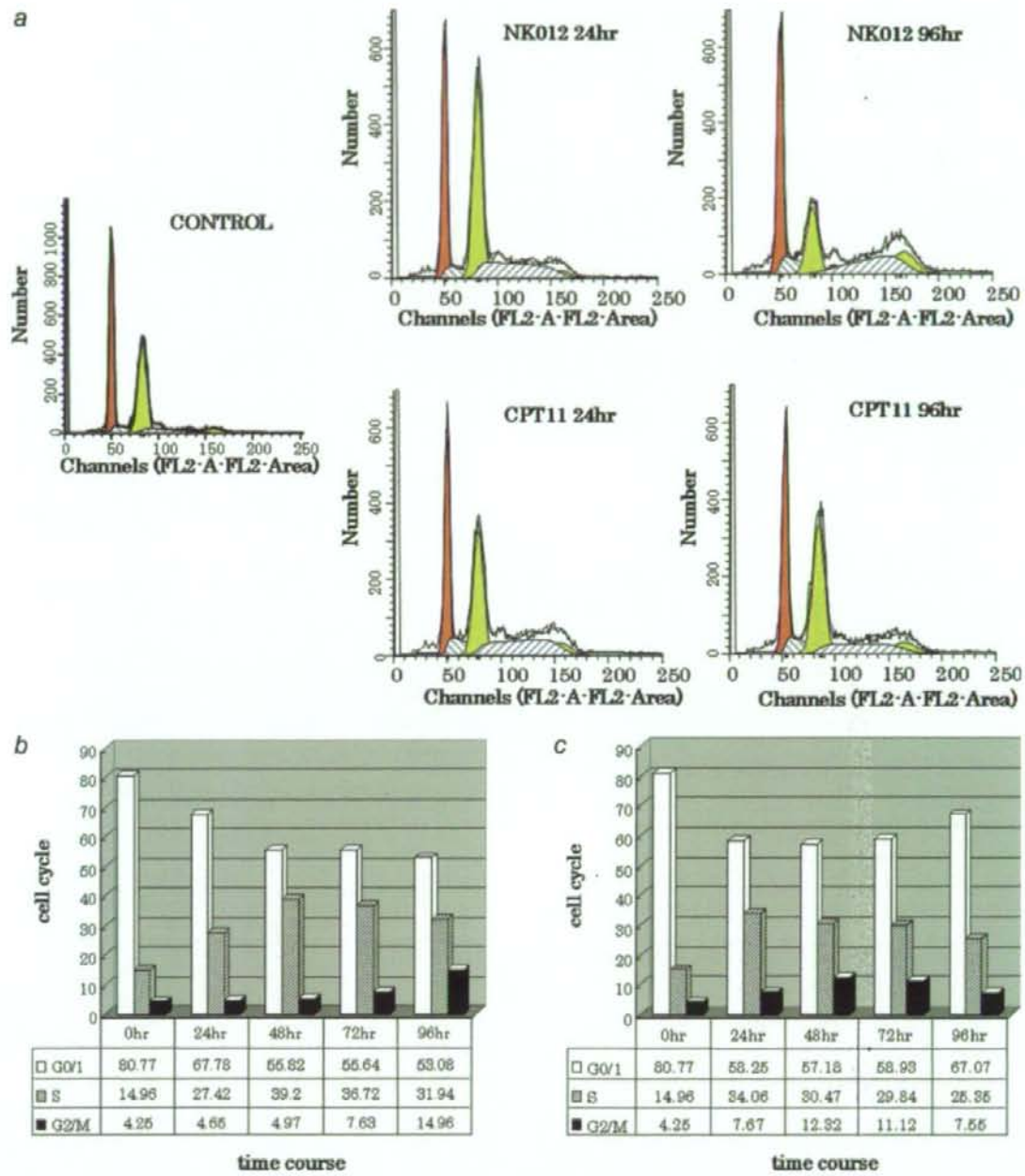

FIGURE 4 – Cell cycle analysis of HT-29 tumor cells collected 24, 48, 72 and 96 hr after administration of NK012 at 10 mg/kg alone or CPT-11 at 50 mg/kg alone using the Modfit program (Verity Software House Topsham, ME). (*a*) Cell cycle analysis of HT-29 tumor cells 24 and 96 hr after administration of NK012 at 10 mg/kg or CPT-11 at 50 mg/kg, respectively. (*b*) Cell cycle distribution of tumor cells 0, 24, 48, 72 and 96 hr after treatment with NK012 at 10 mg/kg. (*c*) Cell cycle distribution of tumor cells 0, 24, 48, 72 and 96 hr after treatment with CPT-11 at 50 mg/kg.

onstrated as compared to that observed with CPT-11 in a rat mammary tumor model.[21] Combined administration of CPT-11 with 5FU/LV infusion appears to be associated with acceptable toxicity in patients with CRC. In addition, no significant difference in the frequency of Grade 3/4 diarrhea was noted between patients treated with FOLFIRI (CPT-11 regimen with bolus and infusional 5FU/LV) and those treated with FOLFOX6 (oxaliplatin regimen with bolus and infusional 5FU/LV).[22,23] Our *in vivo* data actually revealed no severe body weight loss in the NK012/5FU group. Consequently, we expect that the NK012/5FU regimen, especially

with infusional 5FU, may be an attractive arm for a Phase III trial in CRC, with CPT-11/5FU as the control arm. We have already initiated a Phase I trial of NK012 in patients with advanced solid tumors based on the data suggesting higher efficacy and lower toxicity of this preparation than CPT-11 *in vivo*.[12]

In conclusion, we demonstrated that combined NK012 and 5FU chemotherapy exerts significantly greater antitumor activity against human CRC xenografts as compared to CPT-11/5FU, indicating the necessity of clinical evaluation of this combined regimen.

References

1. Saltz LB, Douillard JY, Pirotta N, Alakl M, Gruia G, Awad L, Elfring GL, Locker PK, Miller LL. Irinotecan plus fluorouracil/leucovorin for metastatic colorectal cancer: a new survival standard. Oncologist 2001;6:81–91.
2. Douillard JY, Cunningham D, Roth AD, Navarro M, James RD, Karasek P, Jandik P, Iveson T, Carmichael J, Alakl M, Gruia G, Awad L, et al. Irinotecan combined with fluorouracil compared with fluorouracil alone as first-line treatment for metastatic colorectal cancer: a multicentre randomised trial. Lancet 2000;355:1041–7.
3. Takimoto CH, Arbuck SG. Topoisomerase I targeting agents: the camptothecins. In: Chabner BA, Lango DL, eds. Cancer chemotherapy and biotherapy: principal and practice, 3rd ed. Philadelphia, PA: Lippincott Williams and Wilkins, 2001. 579–646.
4. Slatter JG, Schaaf LJ, Sams JP, Feenstra KL, Johnson MG, Bombardt PA, Cathcart KS, Verburg MT, Pearson LK, Compton LD, Miller LL, Baker DS, et al. Pharmacokinetics, metabolism, and excretion of irinotecan (CPT-11) following I.V. infusion of [(14)C]CPT-11 in cancer patients. Drug Metab Dispos 2000;28:423–33.
5. Rothenberg ML, Kuhn JG, Burris HA, III, Nelson J, Eckardt JR, Tristan-Morales M, Hilsenbeck SG, Weiss GR, Smith LS, Rodriguez GI, Rock MK, Von Hoff DD. Phase I and pharmacokinetic trial of weekly CPT-11. J Clin Oncol 1993;11:2194–204.
6. Guichard S, Terret C, Hennebelle I, Lochon I, Chevreau P, Fretigny E, Selves J, Chatelut E, Bugat R, Canal P. CPT-11 converting carboxylesterase and topoisomerase activities in tumour and normal colon and liver tissues. Br J Cancer 1999;80:364–70.
7. Gradishar WJ, Tjulandin S, Davidson N, Shaw H, Desai N, Bhar P, Hawkins M, O'Shaughnessy J. Phase III trial of nanoparticle albumin-bound paclitaxel compared with polyethylated castor oil-based paclitaxel in women with breast cancer. J Clin Oncol 2005;23:7794–803.
8. Muggia FM. Liposomal encapsulated anthracyclines: new therapeutic horizons. Curr Oncol Rep 2001;3:156–62.
9. Matsumura Y, Maeda H. A new concept for macromolecular therapeutics in cancer chemotherapy: mechanism of tumoritropic accumulation of proteins and the antitumor agent smancs. Cancer Res 1986;46:6387–92.
10. Zhang JA, Xuan T, Parmar M, Ma L, Ugwu S, Ali S, Ahmad I. Development and characterization of a novel liposome-based formulation of SN-38. Int J Pharm 2004;270:93–107.
11. Kraut EH, Fishman MN, LoRusso PM, Gorden MS, Rubin EH, Haas A, Fetterly GJ, Cullinan P, Dul JL, Steinberg JL. Final result of a phase I study of liposome encapsulated SN-38 (LE-SN38): safety, pharmacogenomics, pharmacokinetics, and tumor response [abstract 2017]. Proc Am Soc Clin Oncol 2005;23:139S.
12. Koizumi F, Kitagawa M, Negishi T, Onda T, Matsumoto S, Hamaguchi T, Matsumura Y. Novel SN-38-incorporating polymeric micelles, NK012, eradicate vascular endothelial growth factor-secreting bulky tumors. Cancer Res 2006;66:10048–56.
13. Chou TC, Talalay P. Quantitative analysis of dose-effect relationships: the combined effects of multiple drugs or enzyme inhibitors. Adv Enzyme Regul 1984;22:27–55.
14. Azrak RG, Cao S, Slocum HK, Toth K, Durrani FA, Yin MB, Pendyala L, Zhang W, McLeod HL, Rustum YM. Therapeutic synergy between irinotecan and 5-fluorouracil against human tumor xenografts. Clin Cancer Res 2004;10:1121–9.
15. Jain RK. Barriers to drug delivery in solid tumors. Sci Am 1994; 271:58–65.
16. Savic R, Luo L, Eisenberg A, Maysinger D. Micellar nanocontainers distribute to defined cytoplasmic organelles. Science 2003;300:615–18.
17. Kawato Y, Aonuma M, Hirota Y, Kuga H, Sato K. Intracellular roles of SN-38, a metabolite of the camptothecin derivative CPT-11, in the antitumor effect of CPT-11. Cancer Res 1991;51:4187–91.
18. Slater R, Radstone D, Matthews L, McDaid J, Majeed A. Hepatic resection for colorectal liver metastasis after downstaging with irinotecan improves survival. Proc Am Soc Clin Oncol 2003;22(abstract 1287).
19. Araki E, Ishikawa M, Iigo M, Koide T, Itabashi M, Hoshi A. Relationship between development of diarrhea and the concentration of SN-38, an active metabolite of CPT-11, in the intestine and the blood plasma of athymic mice following intraperitoneal administration of CPT-11. Jpn J Cancer Res 1993;84:697–702.
20. Atsumi R, Suzuki W, Hakusui H. Identification of the metabolites of irinotecan, a new derivative of camptothecin, in rat bile and its biliary excretion. Xenobiotica 1991;21:1159–69.
21. Onda T, Nakamura I, Seno C, Matsumoto S, Kitagawa M, Okamoto K, Nishikawa K, Suzuki M. Superior antitumor activity of NK012, 7-ethyl-10-hydroxycamptoyhecin-incorporating micellar nanoparticle, to irrinotecan. Proc Am Assoc Cancer Res 2006;47:720s(abstract 3062).
22. Tournigand C, Andre T, Achille E, Lledo G, Flesh M, Mery-Mignard D, Quinaux E, Couteau C, Buyse M, Ganem G, Landi B, Colin P, et al. FOLFIRI followed by FOLFOX6 or the reverse sequence in advanced colorectal cancer: a randomized GERCOR study. J Clin Oncol 2004;22:229–37.
23. Colucci G, Gebbia V, Paoletti G, Giuliani F, Caruso M, Gebbia N, Carteni G, Agostara B, Pezzella G, Manzione L, Borsellino N, Misino A, et al. Phase III randomized trial of FOLFIRI versus FOLFOX4 in the treatment of advanced colorectal cancer: a multicenter study of the Gruppo Oncologico Dell'Italia Meridionale. J Clin Oncol 2005; 23:4866–75.

Enhanced distribution of NK012, a polymeric micelle-encapsulated SN-38, and sustained release of SN-38 within tumors can beat a hypovascular tumor

Yohei Saito,[1,2] Masahiro Yasunaga,[1] Junichiro Kuroda,[1] Yoshikatsu Koga[1] and Yasuhiro Matsumura[1,3]

[1]Investigative Treatment Division, Center for Innovative Oncology, National Cancer Center Hospital East, 6-5-1 Kashiwanoha, Kashiwa, Chiba 277-8577; [2]Laboratory of Cancer Biology, Department of Integrated Biosciences, Graduate School of Frontier Sciences, The University of Tokyo, 5-1-5 Kashiwanoha, Kashiwa, Chiba 277-8562, Japan

(Received January 16, 2008/Revised February 14, 2008/Accepted February 14, 2008/Online publication April 21, 2008)

Human pancreatic cancer is generally hypovascular in nature and rich in interstitium. These pathological barriers may contribute to the intractable nature of pancreatic cancer by binding the penetration of anticancer agents throughout the tumor tissue. The aim of the present study was to determine whether NK012 is an appropriate formulation for the treatment of hypovascular tumors. Among pancreatic tumor xenografts, PSN1 appeared to have the richest tumor vasculature and the least number of stromal cells and matrix. In contrast, Capan1 had the poorest tumor vasculature and most abundant stromal tissue. Fluorescence microscopy and high-performance liquid chromatography analysis demonstrated that although NK012 accumulated and continued to be distributed for more than 48 h throughout the entire body of both tumors, CPT-11 disappeared almost entirely from both tumors within 6 h. In addition, efficient sustained release of SN-38 was maintained for more than 96 h in both tumors following administration of NK012. Following the administration of CPT-11, SN-38 was no longer detectable after 24 h in the Capan1 tumor or after 48 h in the PSN1 tumor. All tumors were eradicated in the mice treated with NK012 but not in those treated with CPT-11. Because the antitumor activity of SN-38 is time dependent, NK012, which combines enhanced distribution with sustained release of SN-38 within tumors, may be ideal for the treatment of hypovascular tumors, such as pancreatic cancer. (*Cancer Sci* 2008; 99: 1258–1264)

Pancreatic cancer has one of the worst prognoses among cancers.[1] The median survival of cases of advanced pancreatic cancer is only approximately one in two 1 year after systemic gemcitabine-based chemotherapy.[2] The recent success of molecular-targeting agents has also had some impact on pancreatic cancer treatment. A recent phase III trial of gemcitabine alone versus gemcitabine plus erlotinib (a tyrosine kinase inhibitor) in patients with advanced pancreatic cancer showed that overall survival was significantly prolonged in the gemcitabine + erlotinib arm. However, median survival in the gemcitabine + erlotinib arm (6.24 months) was only 10 days longer than in the gemcitabine-alone arm (5.91 months).[3] There is therefore an urgent need to develop modalities by which cytotoxic drugs can exert their significant antitumor activity to their full potential and reasonably prolong the overall survival of patients with advanced pancreatic cancer. There may be several reasons why pancreatic cancer is intractable. It is conceivable that anticancer agents are not delivered efficiently enough to the pancreatic cancer cells to kill them. Pancreatic cancer tissue is generally hypovascular in nature,[4,5] and is rich in stromal cells and extracellular matrix, and these pathological barriers may hinder efficient penetration of the anticancer agents throughout the entire body of the pancreatic cancer.

The role of drug delivery systems (DDS) is to selectively deliver cytotoxic drugs to tumor tissues while lessening their distribution to normal tissues in order to reduce their side effects.[6–8] However, it is conceivable that satisfactory drug delivery cannot be achieved in cancers having very few tumor vessels and an abundant collagen-rich interstitium. Therefore, a more sophisticated DDS may be needed for efficient delivery of drugs to such types of cancer as pancreatic cancer.

SN-38, a biologically active metabolite of irinotecan hydrochloride (CPT-11), has potent antitumor activity but has not been used clinically because of its water insolubility. NK012, a successful drug formulation composed of SN-38-incorporating polymeric micelles, has been developed recently, and the remarkable antitumor effects of NK012 against the human small cell lung cancer SBC-3, especially the vascular endothelial growth factor (VEGF)-secreting SBC-3–VEGF tumor, has been demonstrated.[8]

In the present study, we clarified the relationship between the tumor vasculature and interstitium using several human pancreatic xenografts, and evaluated the therapeutic effect of NK012 in a hypovascular and hypervascular pancreatic tumor.

Materials and Methods

Drugs and cells. SN-38 and NK012 were synthesized by Nippon Kayaku (Tokyo, Japan). CPT-11 was purchased from Yakult (Tokyo, Japan). The human pancreatic cancer cell lines Panc1, PSN1, BxPC3, and Capan1 were purchased from American Type Culture Collection (Rockville, MD, USA).

Panc1, PSN1, and Capan1 were maintained in Dulbecco's modified Eagle's medium (DMEM) supplemented with 10% fetal bovine serum, streptomycin, and L-glutamine (Sigma, St Louis, MO, USA) in atmosphere of 5% CO_2 at 37°C. BxPC3 were maintained in RPMI-1640 supplemented with 10% fetal bovine serum, streptomycin, and L-glutamine (Sigma) in an atmosphere of 5% CO_2 at 37°C.

Experimental mouse model. Female BALB/c nude mice, 6 weeks old, were purchased from CLEA Japan (Tokyo, Japan). Mice were inoculated subcutaneously in the flank with 1×10^7 cells/300 μL phosphate-buffered saline (PBS). All animal procedures were carried out in compliance with the guidelines for the care and use of experimental animals, laid down by the Committee for Animal Experimentation of the National Cancer Center; these guidelines meet the ethical standards required by law and also comply with the guidelines for the use of experimental animals in Japan.

[3]To whom correspondence should be addressed. E-mail: yhmatsum@east.ncc.go.jp

doi: 10.1111/j.1349-7006.2008.00806.x

Immunohistochemical study of various human pancreatic tumor xenografts. When the tumor volume reached 300 mm^3, tumors were excised from the mice and used for immunohistochemical analysis. To stain the blood vessels, the tissues were embedded in Optimal Cutting Temperature Compound (Sakura Finetechnochemical, Tokyo, Japan) and frozen at –80°C until use. Six micrometer-thick tumor sections were prepared using a cryostatic microtome, Tissue-Tek Cryo3 (Sakura Finetechnochemical), and then air dried for 1 h. The sections were soaked in 10% formalin for 15 min, and washed three times with 0.2 M PBS. The sections were then rinsed with ultrapure water. Endogeneous peroxidase was blocked with a 0.3% hydrogen peroxide solution in 100% methanol for 20 min. The sections were then rinsed three times with PBS for 3 min each. Non-specific protein binding was blocked with 5% skim milk (BD, Franklin Lakes, NJ, USA) in PBS for 30 min at room temperature. After draining off the skim milk solution, a polyclonal antibody against factor VIII (Zymed Laboratories, South San Francisco, CA, USA) was added at a dilution of 1:50, followed by incubation for 1 h and three rinses with PBS for 5 min each. Biotinylated antirabbit IgG was added at a dilution of 1:50, followed by incubation for 1 h. The sections were rinsed three times with PBS, and Vectastain Elite ABC Reagent (Vector Laboratories, Burlingame, CA, USA) was added for 30 min. The sections were rinsed again three times with PBS and incubated with the 3,3′-diaminobenzidine tetrahydrochloride (DAB+) Liquid System (Dako, Glostrup, Denmark) for 30 s. Finally, the sections were rinsed and counterstained with hematoxylin solution. For staining of type I, III, and IV collagen, tissues were fixed with 4% formalin, and the paraffin sections were prepared by the Tokyo Histopathologic Laboratory (Tokyo, Japan). First, the sections were soaked three times for 5 min each in xylene, and then three times for 3 min each in ethanol to remove the paraffin. The sections were then rinsed with ultrapure water and endogeneous peroxidase was blocked with a 0.3% hydrogen peroxide solution in 100% methanol for 20 min, followed by three rinses for 5 min with PBS. Then, Proteinase K (Dako) was added. After the sections were rinsed three times for 5 min each with 0.2 M PBS, non-specific protein binding was blocked with a 1% normal goat serum (Dako) solution in PBS for 30 min at room temperature. Then, after three rinses for 5 min each with PBS, polyclonal rabbit anti type I, III, and IV collagen antibodies (Dako) were added at dilutions of 1:500 (type I collagen), 1:10 000 (type III collagen), and 1:2000 (type IV collagen), followed by incubation for 1 h. The slides were rinsed in PBS and incubated for 30 min with Envision/HRP (Dako) directed against the primary antibody. After further rinsing, the sections were incubated with the DAB+ Liquid System (Dako) for 30 s. Then, after a final rinse, the sections were counterstained with hematoxylin solution.

***In vitro* growth assay.** The growth-inhibitory effects of NK012, SN-38, and CPT-11 were examined using the WST8 assay. Cell suspensions (5000 cells/100 μL) were seeded into a 96-well microliter plate, which was incubated for 24 h at 37°C. Then, after removal of the medium, 100 μL of medium containing various concentrations of each drug was added to the wells, which were then incubated for 48 h at 37°C. After removal of the medium, 10 μL of WST8 solution and 90 μL of medium were added to the wells, followed by incubation for 4 h at 37°C. The growth-inhibitory effect of each drug was assessed spectrophotometrically (SpectraMax 190; Molecular Devices, Sunnyvale, CA, USA).

Distribution studies of CPT-11 and NK012 in the tumors by fluorescence microscopy. Nude mice bearing PSN1, as a hypervascular tumor model, or Capan1, as a hypovascular tumor model, were used for studying the distribution of NK012 and CPT-11, when the tumors reached 300 mm^3 in volume. The maximum tolerated dose (MTD) of NK012 (30 mg/kg) or CPT-11 (66.7 mg/kg) was injected intravenously into the mice. At 1, 6, 24, or 48 h after the injection of NK012 or CPT-11, the mice were administered fluorescein-labeled *Lycopersicon esculentum* lectin (100 μL/mouse) (Vector Laboratories) for the purpose of visualizing the tumor blood vessels. The tumors were then excised and embedded in Optimal Cutting Temperature Compound and frozen at –80°C before 6 μm-thick sections were prepared using Tissue-Tek Cryo3. The frozen sections were examined under a fluorescence microscope, Biorevo (Keyence, Osaka, Japan), at an excitation wavelength of 377 nm and emission wavelength 447 nm in order to evaluate the distribution of CPT-11 and NK012 within the tumor tissues. Because formulations containing SN-38 bound via ester bonds possess a particular fluorescence, both CPT-11 and NK012 were detected under the same fluorescence conditions.

Distribution studies of free SN-38, CPT-11, and NK012 in the tumors by high-performance liquid chromatography. When PSN1 and Capan1 tumors reached 300 mm^3 in volume, NK012 (30 mg/kg) or CPT-11 (66.7 mg/kg) was administered intravenously to the mice. At 1, 6, 24, 72, or 96 h after the injection of NK012 and CPT-11, each tumor was excised. The tumor tissues were rinsed with physiological saline, mixed with 0.1 M glycine-HCl buffer (pH 3.0) in methanol at 5% (w/w) and homogenized. To detect free SN-38 and CPT-11, the tumor samples (100 μL) were mixed with 20 μL of 1 mM phosphoric acid in methanol (1:1), 40 μL ultrapure water, and camptothecin was used as the internal standard (10 ng/mL for free SN-38, 15 ng/mL for CPT-11). The samples were vortexed vigorously for 10 s and filtered through Ultrafree-MC Centrifugal Filter Devices (Millipore, Bedford, MA, USA). Reverse-phase high-performance liquid chromatography (HPLC) was conducted at 35°C on a Mightysil RP-18 GP column (150 × 4.6 mm; Kanto Chemical, Tokyo, Japan). The samples were injected into an Alliance Water 2795 HPLC system (Waters, Milford, MA, USA) equipped with a Waters 2475 multi λ fluorescence detector. The detector was set at 365 and 430 nm (excitation and emission wavelengths, respectively) for CPT-11, and at 365 and 540 nm for SN-38.

For polymer-bound SN-38 detection, SN-38 was released from the conjugate as described previously.[8] In brief, 100 μL tissue samples were diluted with 20 μL methanol (50% [w/w]) and 20 μL NaOH (0.7 M). The samples were incubated for 15 min at room temperature. After incubation, 20 μL HCl (0.7 M) and 60 μL of internal standard solution was added to the samples, and then the hydrolysate was filtered. The filtrate was applied to the HPLC system.

Polymer-bound SN-38 was determined by subtraction of non-polymer-bound SN-38 from the total SN-38 in the hydrolysate.

Antitumor activity of NK012 and CPT-11 against Capan1 or PSN1 xenografts. When the tumor volume reached approximately 300 mm^3 in volume, the mice were divided randomly into test groups consisting of five mice per group (day 0). The drugs were administered on days 0, 4, and 8 by intravenous injection into the tail vein. NK012 was given at a dose of 30 mg/kg (MTD) and CPT-11 was given at a MTD of 66.7 mg/kg as indicated in the optimal schedule reported previously.[9]

The length (L) and width (W) of the tumor mass were measured every 3 days. The tumor volume (TV) was calculated as follows: $TV = (L \times W^2) \times 0.5233$.

Statistical analysis. Student's *t*-test was used for the statistical analyses. $P < 0.05$ was considered to denote statistical significance.

Results

Density of collagen and the number of tumor blood vessels in the various human pancreatic tumor xenografts. We examined the density of collagen in four pancreatic cancer xenografts (Fig. 1a). Type I collagen was present in the greatest abundance in Capan1 and was least abundance in PSN1. The density of type I collagen in Panc1 and BxPC3 was in second and third place, respectively.

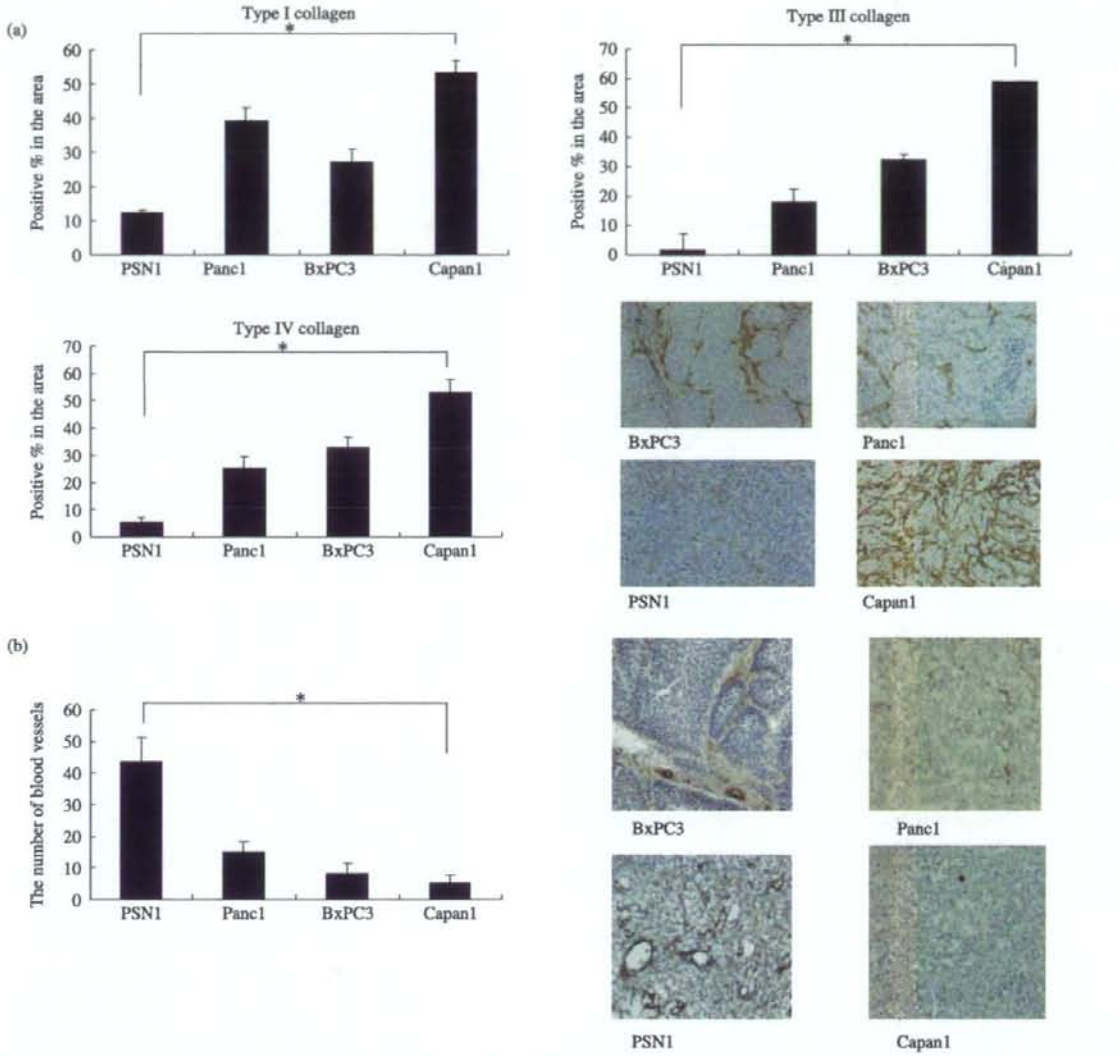

Fig. 1. Examination of the amount of stroma and the number of tumor blood vessels in four human pancreatic cancer xenografts. (a) The amount of stroma in the four xenografts BxPC3, Panc1, PSN1, and Capan1. Immunohistochemical staining was conducted in order to determine the distribution of type I, III, and IV collagen in the tumors. The area occupied by each of type I collagen (left, upper), type III collagen (right, upper), and type IV collagen (left, bottom) was quantified. A representative immunostained image for type IV collagen is shown (right, bottom). (b) The number of blood vessels in the four xenografts. After immunostaining with anti-factor VIII antibody, the number of tumor blood vessels in each of the xenografts was counted. $*P < 0.05$. Bar = SD.

Capan1 exhibited the highest density of type III collagen, and BxPC3 and PSN1 were in second and fourth place, respectively, with respect to the density of type III collagen. The distribution of type IV collagen tended to be similar to that of type I and III collagen.

We also examined the number of tumor blood vessels (Fig. 1b). The PSN1 tumor possessed the largest number of blood vessels among the tumors. In contrast, the Capan1 xenografts had the smallest number of tumor blood vessels.

We have summarized the results on collagen density and blood vessel number obtained in our study for each pancreatic xenograft. Capan1 was the most collagen-rich tumor, and the density of collagen was lowest in PSN1. In contrast, tumor blood vessels were most abundant in PSN1 and least abundant in Capan1. Therefore, we decided to use Capan1 as a hypovascular tumor model and PSN1 as a hypervascular tumor model.

***In vitro* cytotoxic effects of NK012, SN-38, and CPT-11 against the Capan1 and PSN1 cell lines.** The 50% inhibitory concentration (IC_{50}) values of NK012 for the two cell lines, Capan1 (Fig. 2a) and PSN1 (Fig. 2b), ranged from 0.001 to 0.1 μM. NK012 exhibited a remarkably higher cytotoxic effect against both of the cell lines compared with CPT-11. In contrast the cytotoxic effect of SN-38 was similar to that of NK012. The IC_{50} value of each drug against PSN1 was almost similar to that of Capan1.

Antitumor activity analysis of NK012 and CPT-11 using Capan1- and PSN1-bearing nude mice. Antitumor activity was observed in mice treated with NK012 at a dose of 30 mg/kg/d and CPT-11

doi: 10.1111/j.1349-7006.2008.00806.x

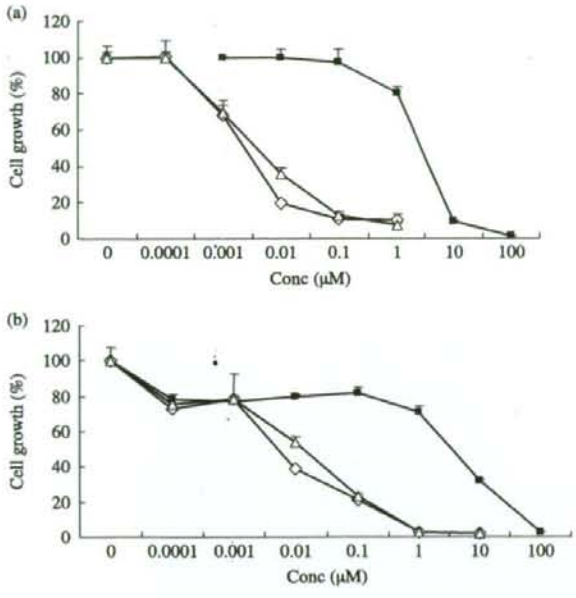

Fig. 2. (a) Capan1 and (b) PSN1 cells were exposed to the indicated concentrations of each drug for 72 h. The growth inhibition curves for NK012 (△), SN-38 (◇), and CPT-11 (■) are shown.

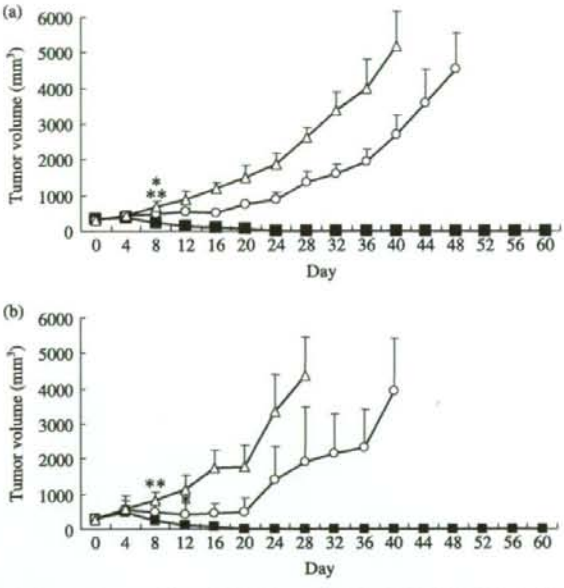

Fig. 3. Antitumor effect of NK012 and CPT-11. NK012 (■), CPT-11 (○), or saline (△) was administered intravenously. When the mean tumor volumes reached 300 mm³ (on day 0), NK012 (30 mg/kg/day) or CPT-11 (66.7 mg/kg/day) was administered on days 0, 4, and 8. Each group consisted of five mice. (a) Capan1 tumor; (b) PSN1 tumor. $*P < 0.05$ (NK012 vs CPT11); $**P < 0.05$ (NK012 vs saline).

at a dose of 66.7 mg/kg/d *in vivo* (Fig. 3). Although CPT-11 exerted a significant antitumor effect compared with the control group in mice bearing the Capan1 tumor, the tumor volume continued to increase consistently. However, in the mice treated with NK012, the tumor volume started to shrink on day 8, and the disappeared completely by day 28 in all treated mice bearing the Capan1 tumor.

In contrast to the observations for the Capan1 tumor, mice bearing the PSN1 tumor treated with CPT-11 showed a slight reduction in tumor volume from day 4 to 12. However, after day 12 the tumor volume began to increase again. On the other hand, the tumor disappeared completely in all mice bearing the PSN1 tumor treated with NK012.

Distribution studies of CPT-11 and NK012 in the solid Capan1 and PSN1 tumors. With the purpose of evaluating drug distribution and accumulation over time, sections of the tumor treated with NK012 or CPT-11 were examined by fluorescence microscopy. Also, we examined the number of tumor blood vessels. In sections of the Capan1 tumor treated with CPT-11, maximum drug accumulation was observed within 1 h of the injection of CPT-11 (Fig. 4a). At 6 h after the injection, the fluorescence originating from CPT-11 had almost entirely disappeared. Subsequently, no accumulation of CPT-11 was observed within the tumor tissues. However, in sections of the Capan1 tumor treated with NK012, fluorescence from NK012 began to appear around tumor blood vessels at 1 h after the intravenous injection and lasted until 48 h. After 6 h, the fluorescent area began to increase and the maximum fluorescence area was observed at 24 h after the injection. Similar results were obtained for the PSN1 tumor (Fig. 4b).

These microscopic observations were confirmed quantitatively by measuring the amount of SN-38 that could be extracted from each of the solid tumors by reverse-phase HPLC. Only slight conversion from CPT-11 to SN-38 was seen from 1 to 24 h in the Capan1 tumor and from 1 to 48 h in the PSN1 tumor, and no SN-38 was detected thereafter. In contrast, SN-38 released from NK012 continued to be detected in both tumors from 1 to 96 h after the injection of NK012 (Fig. 5).

Discussion

Recently, several new formulations categorized as DDS have been approved in the field of oncological treatment, such as Doxil, a polyethylene glycol-liposome incorporating adriamycin,[10,11] and abraxane, a taxol coated with albumin.[12,13] In addition, several clinical trials of drugs based on the DDS concept are now underway.[14–16] Because such formulations possess a longer plasma area under the curve (AUC), liposomal drugs should have sufficient time to exit from tumor blood vessel and accumulate at reasonably high dose levels in the surrounding interstitium.

It has been reported that although polyethylene glycol (PEG) liposomes can be delivered efficiently to a solid tumor, free drug is not transferred sufficiently to cancer cells, particularly those that are distant from the tumor vessels, because the formulations are too large to move through the tumor interstitium.[17] Also, it has been suggested that liposomes are too stable to allow the drug within to be released easily. Therefore, it has been speculated that PEG liposomes may not be so effective against cancers in which the tumor vessel network is irregular and loose because of an abundant collagen-rich matrix. Some examples of such cancers include scirrhous cancer of the stomach and pancreatic cancer. In fact, Doxil is known to be clinically effective against ovarian and breast cancers, both of which are characterized by a high density of tumor microvessels, whereas it is not effective against stomach and pancreatic cancers.[18] Therefore, it is conceivable that some special device is necessary for DDS drugs to exert their antitumor effect sufficiently even against hypovascular tumors such as pancreatic cancer.

In the present study, we characterized the tumor vessel and its interstitium using four kinds of human pancreatic xenografts. The results revealed that the number of tumor blood vessels was inversely related to the amount of collagen within the tumor tissues. Among the four cell lines, Capan1 was the poorest in

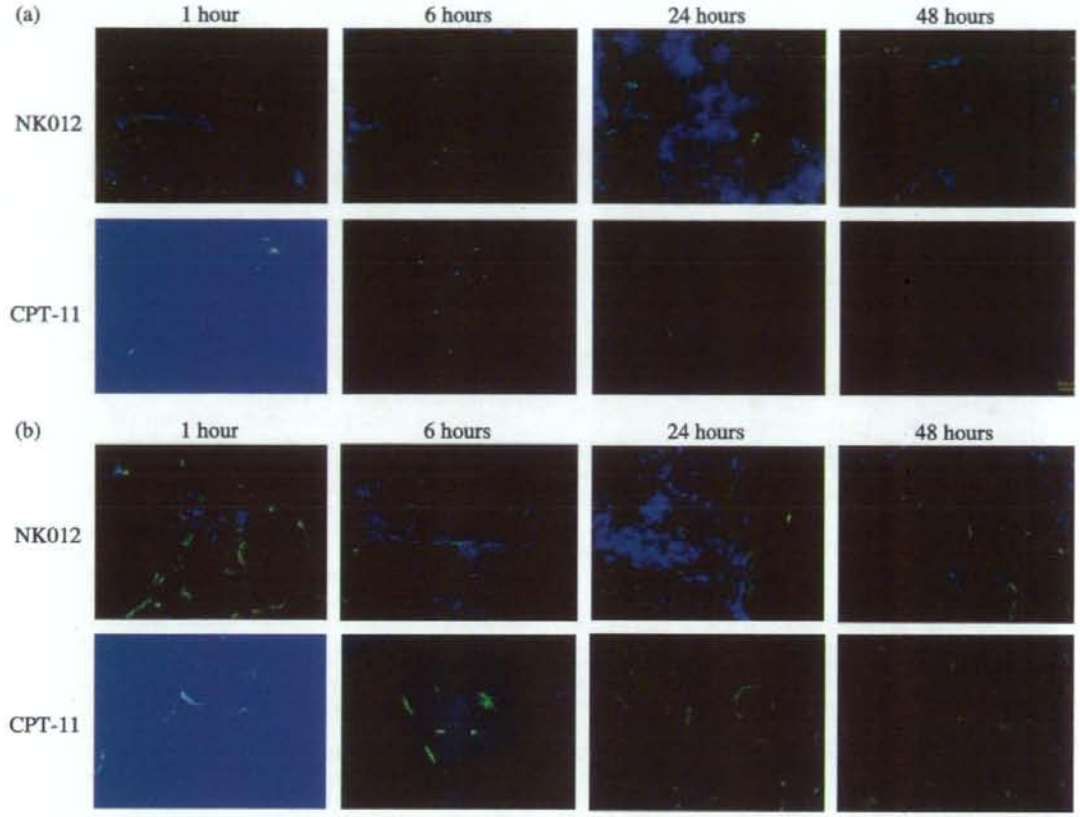

Fig. 4. Distribution of NK012 or CPT-11 in the (a) Capan1 and (b) PSN1 tumor xenografts. Mice bearing Capan1 or PSN1 tumors were injected with NK012 (30 mg/kg/day) or CPT-11 (66.7 mg/kg/day). The tumor tissues were excised at 1, 6, 24, and 48 h after the intravenous injection of NK012 or CPT-11. Each mouse was administered an injection of fluorescein-labeled *Lycopersicon esculentum* lectin just before being killed, for detecting the tumor blood vessels. The frozen sections were examined under a fluorescence microscope at an excitation wavelength of 377 nm and emission wavelength of 447 nm. The same fluorescence conditions can be applied for visualizing NK012 and CPT-11 fluorescence. Free SN-38 can not be detected under these fluorescence conditions.

tumor vasculature and richest in the amount of collagen within the tumor tissue. Conversely, PSN1 was the richest in tumor vasculature and poorest in the amount of collagen. Therefore, it may safely be said that Capan1 xenografts are most like human pancreatic cancer tissue in terms of the amount of interstitial tissue among the four cell lines tested.

We evaluated the *in vitro* cytotoxic effect of CPT-11, SN-38, and NK012 and the *in vivo* antitumor activity of CPT-11 and NK012 against Capan1 tumors as a hypovascular tumor model and PSN1 tumors as a hypervascular tumor model. SN-38 and NK012 exhibited a higher cytotoxic effect against the two cell lines compared with CPT-11. Between SN-38 and NK012, the cytotoxic effect of NK012 was almost similar or a little lower compared with that of SN-38. As CPT-11 itself is a prodrug and is converted to SN-38, an active metabolite of CPT-11, by carboxylesterases, the activity of CPT-11 is dependent on the activity of the enzymes. It is speculated that the efficient sustained release of SN-38 from NK012 allows the formulation to exert a similar cytotoxic effect to that of SN-38. In the *in vivo* experiment, CPT-11 showed significant antitumor activity against both PSN1 tumors as a hypervascular tumor model and Capan1 tumors as a hypovascular tumor model. A slight reduction in tumor size was observed from day 4 to 12 in the case of PSN1 tumors, but not Capan1 tumors. We suggest that the higher antitumor activity seen in PSN1 compared with Capan1 tumors is probably because of the greater accumulation of CPT-11 in the PSN1 xenografts because of the more abundant vasculature. Surprisingly, NK012 could cause complete disappearance of both PSN1 and Capan1 tumor xenografts. Before conducting the experiment, we had anticipated that NK012 might exert stronger antitumor effects against PSN1 compared with Capan1, because such macromolecular drugs can accumulate more efficiently in the PSN1 xenografts because of the richer vasculature. Therefore, we then intensively examined the distribution of NK012 and CPT-11 within the PSN1 or Capan1 xenografts by fluorescence microscopy and HPLC. In the analysis by fluorescence microscopy, NK012 appeared within and around the tumor blood vessels in both the PSN1 and Capan1 xenografts at 1 h after the injection. NK012 began to spread from the blood vessels within the tumor tissue of both xenografts. Fluorescence originating from NK012 increased to a maximum in both of the tumors by 24 h after the injection of NK012. Namely, NK012 was distributed throughout the entire body of both tumors at 24 h after the injection. Furthermore, fluorescence originating from NK012 was clearly and diffusely detected throughout both tumors.

However, fluorescence originating from CPT-11 increased to a maximum at 1 h in both tumors after the injection of CPT-11, indicating that maximum distribution of CPT-11 was achieved

doi: 10.1111/j.1349-7006.2008.00806.x

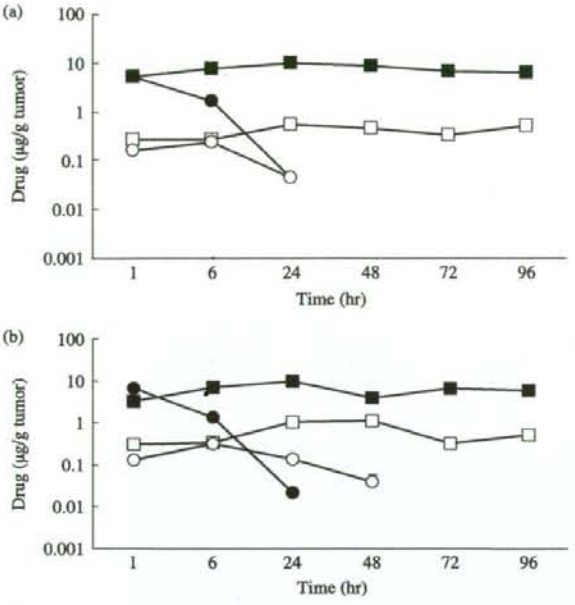

Fig. 5. Tumor distribution of CPT-11, NK012 (or polymer bound SN-38), and free SN-38 after administration of NK012 and CPT-11 to mice bearing (a) Capan1 or (b) PSN1 xenografts. The time profiles of polymer-bound SN-38 (■), free SN-38 released from NK012 (□), CPT-11 (●), and free SN-38 converted from CPT-11 (○) were obtained by high-performance liquid chromatography analysis. The time points examined were 1, 6, 24, 48, 72, and 96 h after the administration of CPT-11 or NK012.

in both tumors within 1 h of the injection. No or very slight fluorescence of CPT-11 was observed in the tumors at 6 h after CPT-11 injection. These observations were confirmed quantitatively by measuring the amount of SN-38 extracted from both tumors by reverse-phase HPLC. Only slight conversion to SN-38 from CPT-11 was seen from 1 to 24 h in the Capan1 tumor and from 1 to 48 h in the PSN1 tumor, and no SN-38 was detected thereafter. SN-38 released from NK012 continued to be detected in both tumors from 1 to 96 h after the injection of NK012. In both CPT-11 and NK012, SN-38 binds to each counter molecule via an ester bond, which confers blue fluorescence on CPT-11 and NK012. Therefore, it is speculated that polymer-bound SN-38 can be distributed throughout the entire body of the tumor, regardless of the amount of interstitial tissue. We are unable to explain clearly how NK012 was distributed well even in hypovascular tumors. However, it is speculated that NK012 can move smoothly within the tumor interstitium because of its relatively small particle size (20 nm) compared with other DDS formulations, and because of its flexibility the formulation can pass through even narrow gaps within the interstitium. Previously, we reported that sustained release of 74% free SN-38 occurred from NK012 under physiological conditions within 48 h.[8] It is also important to remember that the antitumor activity of SN-38 is time dependent.[19] Taking all of these data together, it may be concluded that NK012 can selectively accumulate in pancreatic tumor xenografts, to be distributed effectively throughout the entire body of the tumor, including in hypovascular tumors, and shows sustained release for a prolonged period of time. Consequently, NK012 can exert more significant antitumor activity than CPT-11, which is not an ideal formulation for realizing the time-dependent actions of the drug.

In addition to our present study, there have been several efforts to enhance the accumulation of anticancer agents in tumors to obtain higher antitumor activities of drugs. For example, it has been reported that a transforming growth factor-β inhibitor can enhance tumor vascular permeability to promote accumulation of macromolecules.[20] Conversely, combined use of an antiangiogenic agent, such as an antibody to VEGF, with an anticancer agent could enhance the antitumor activity, probably by lowering the tumor vascular permeability with a consequent decrease in the interstitial fluid pressure so that the anticancer agents may accumulate more easily in the tumor.[21,22] However, much remains to be clarified.

In the present paper, we have shown not only the superiority of the antitumor effect of NK012 compared with that of CPT-11, but also propose that enhanced accumulation, distribution, and retention of DDS within the tumor tissue and the sustained release of anticancer agents from DDS particles are key elements for the treatment of hypovascular tumors. A phase I clinical trial is now underway. Not only the clinical usefulness of NK012, but also the new concept for antitumor actions described in this paper are intended to be verified in the near future through further preclinical and clinical studies.

Acknowledgments

We thank Mrs H. Miyatake and Mrs N. Mie for their technical assistance and Mrs K. Shiina for her secretarial assistance. This work was supported partly by a Grant-in-Aid from the 3rd Term Comprehensive Control Research for Cancer, Ministry of Health, Labor and Welfare (Y. Matsumura) and Scientific Research on Priority Areas from the Ministry of Education, Culture, Sports, Science and Technology (Y. Matsumura).

References

1 Jemal A, Siegel R, Ward E, Murray T, Xu J, Thun MJ. Cancer statistics, 2007. *CA Cancer J Clin* 2007; **57**: 43–66.
2 Burris HA 3rd, Moore MJ, Andersen J *et al.* Improvements in survival and clinical benefit with gemcitabine as first-line therapy for patients with advanced pancreas cancer: a randomized trial. *J Clin Oncol* 1997; **15**: 2403–13.
3 Moore MJ, Goldstein D, Hamm J *et al.* Erlotinib plus gemcitabine compared with gemcitabine alone in patients with advanced pancreatic cancer: a phase III trial of the National Cancer Institute of Canada Clinical Trials Group. *J Clin Oncol* 2007; **25**: 1960–6.
4 Hosoki T. Dynamic CT of pancreatic tumors. *AJR Am J Roentgenol* 1983; **140**: 959–65.
5 Sofuni A, Iijima H, Moriyasu F *et al.* Differential diagnosis of pancreatic tumors using ultrasound contrast imaging. *J Gastroenterol* 2005; **40**: 518–25.
6 Matsumura Y, Maeda H. A new concept for macromolecular therapeutics in cancer chemotherapy: mechanism of tumoritropic accumulation of proteins and the antitumor agent smancs. *Cancer Res* 1986; **46**: 6387–92.
7 Muggia FM. Doxorubicin-polymer conjugates: further demonstration of the concept of enhanced permeability and retention. *Clin Cancer Res* 1999; **5**: 7–8.
8 Koizumi F, Kitagawa M, Negishi T *et al.* Novel SN-38-incorporating polymeric micelles, NK012, eradicate vascular endothelial growth factor-secreting bulky tumors. *Cancer Res* 2006; **66**: 10 048–56.
9 Kawato Y, Furuta T, Aonuma M, Yasuoka M, Yokokura T, Matsumoto K. Antitumor activity of a camptothecin derivative, CPT-11, against human tumor xenografts in nude mice. *Cancer Chemother Pharmacol* 1991; **28**: 192–8.
10 Muggia FM. Liposomal encapsulated anthracyclines: new therapeutic horizons. *Curr Oncol Rep* 2001; **3**: 156–62.
11 Ferrari M. Cancer nanotechnology: opportunities and challenges. *Nat Rev Cancer* 2005; **5**: 161–71.
12 Green MR, Manikhas GM, Orlov S *et al.* Abraxane, a novel Cremophor-free, albumin-bound particle form of paclitaxel for the treatment of advanced non-small-cell lung cancer. *Ann Oncol* 2006; **17**: 1263–8.
13 Gradishar WJ, Tjulandin S, Davidson N *et al.* Phase III trial of nanoparticle albumin-bound paclitaxel compared with polyethylated castor oil-based paclitaxel in women with breast cancer. *J Clin Oncol* 2005; **23**: 7794–803.
14 Matsumura Y, Hamaguchi T, Ura T *et al.* Phase I clinical trial and pharmacokinetic evaluation of NK911, a micelle-encapsulated doxorubicin. *Br J Cancer* 2004; **91**: 1775–81.

15 Hamaguchi T, Matsumura Y, Suzuki M *et al*. NK105, a paclitaxel-incorporating micellar nanoparticle formulation, can extend *in vivo* antitumour activity and reduce the neurotoxicity of paclitaxel. *Br J Cancer* 2005; **92**: 1240–6.
16 Uchino H, Matsumura Y, Negishi T *et al*. Cisplatin-incorporating polymeric micelles (NC-6004) can reduce nephrotoxicity and neurotoxicity of cisplatin in rats. *Br J Cancer* 2005; **93**: 678–87.
17 Unezaki S, Maruyama K, Hosoda J *et al*. Direct measurement of the extravasation of polyethylene glycol-coated liposomes into solid tumour tissue by *in vivo* fluorescence microscopy. *Int J Pharmacol* 1996; **144**: 11–17.
18 Tsukioka Y, Matsumura Y, Hamaguchi T, Koike H, Moriyasu F, Kakizoe T. Pharmaceutical and biomedical differences between micellar doxorubicin (NK911) and liposomal doxorubicin (Doxil). *Jpn J Cancer Res* 2002; **93**: 1145–53.
19 Kawato Y, Aonuma M, Hirota Y, Kuga H, Sato K. Intracellular roles of SN-38, a metabolite of the camptothecin derivative CPT-11, in the antitumor effect of CPT-11. *Cancer Res* 1991; **51**: 4187–91.
20 Kano MR, Bae Y, Iwata C *et al*. Improvement of cancer-targeting therapy, using nanocarriers for intractable solid tumors by inhibition of TGF-β signaling. *Proc Natl Acad Sci USA* 2007; **104**: 3460–5.
21 Jain RK. Normalizing tumor vasculature with anti-angiogenic therapy: a new paradigm for combination therapy. *Nat Med* 2001; **7**: 987–9.
22 Jain RK. Normalization of tumor vasculature: an emerging concept in antiangiogenic therapy. *Science* 2005; **307**: 58–62.

doi: 10.1111/j.1349-7006.2008.00806.x

Drug Metab. Pharmacokinet. 23 (2): *SNP1* (139)–*SNP9* (147) (2008).

SNP Communication

Genetic Variations and Haplotypes of *ABCC2* Encoding MRP2 in a Japanese Population

Kimie SAI[1,2,*], Yoshiro SAITO[1,2], Masaya ITODA[1], Hiromi FUKUSHIMA-UESAKA[1], Tomoko NISHIMAKI-MOGAMI[2], Shogo OZAWA[1,3,a], Keiko MAEKAWA[1,2], Kouichi KUROSE[1,4], Nahoko KANIWA[1,4], Manabu KAWAMOTO[5], Naoyuki KAMATANI[5], Kuniaki SHIRAO[6,b], Tetsuya HAMAGUCHI[6], Noboru YAMAMOTO[6], Hideo KUNITOH[6], Yuichiro OHE[6], Yasuhide YAMADA[6], Tomohide TAMURA[6], Teruhiko YOSHIDA[7], Hironobu MINAMI[8,c], Yasuhiro MATSUMURA[9], Atsushi OHTSU[10], Nagahiro SAIJO[11] and Jun-ichi SAWADA[1,2]

[1]*Project Team for Pharmacogenetics,* [2]*Division of Functional Biochemistry and Genomics,*
[3]*Division of Pharmacology,* [4]*Division of Medicinal Safety Science,*
National Institute of Health Sciences, Tokyo, Japan
[5]*Division of Genomic Medicine, Department of Advanced Biomedical Engineering and Science, Tokyo Women's Medical University, Tokyo, Japan*
[6]*Division of Internal Medicine, National Cancer Center Hospital*
[7]*Genomics Division, National Cancer Center Research Institute, National Cancer Center, Tokyo, Japan*
[8]*Division of Oncology/Hematology,*
[9]*Investigative Treatment Division, Research Center for Innovative Oncology,*
[10]*Division of GI Oncology/Digestive Endoscopy,*
[11]*Deputy Director, National Cancer Center Hospital East, Chiba, Japan*

Full text of this paper is available at http://www.jstage.jst.go.jp/browse/dmpk

Summary: The multidrug resistance-associated protein 2 (MRP2) encoded by the *ABCC2* gene is expressed in the liver, intestine and kidneys and preferentially exports organic anions or conjugates with glucuronide or glutathione. In this study, all 32 exons and the 5′-flanking region of *ABCC2* in 236 Japanese were resequenced, and 61 genetic variations including 5 novel nonsynonymous ones were detected. A total of 64 haplotypes were determined/inferred and classified into five *1 haplotype groups (*1A, *1B, *1C, *1G, and *1H) without nonsynonymous substitutions and *2 to *9 groups with nonsynonymous variations. Frequencies of the major 4 haplotype groups *1A (−1774delG), *1B (no common SNP), *1C (−24C>T and 3972C>T), and *2 [1249G>A (Val417Ile)] were 0.331, 0.292, 0.172, and 0.093, respectively. This study revealed that haplotype *1A, which has lowered activity, is quite common in Japanese, and that the frequency of *1C, another functional haplotype, was comparable to frequencies in Asians and Caucasians. In contrast, the haplotypes harboring 3972C>T but not −24C>T (*1G group), which are reportedly common in Caucasians, were minor in Japanese. Moreover, the allele 1446C>T (Thr482Thr), which has increased activity, was not detected in our Japanese population. These findings imply possible differences in MRP2-mediated drug responses between Asians and Caucasians.

Keywords: ABCC2; MRP2; genetic variation; haplotype; amino acid change

Received; October 15, 2007, Accepted; December 5, 2007

**To whom correspondence should be addressed:* Kimie SAI, Ph.D., *Division of Functional Biochemistry and Genomics, National Institute of Health Sciences, 1-18-1 Kamiyoga, Setagaya-ku, Tokyo 158-8501, Japan. Tel: +81-3-3700-9478, Fax: +81-3-3707-6950, E-mail: sai@nihs.go.jp*
[a]Present address: Department of Pharmacodynamics and Molecular Genetics, Faculty of Pharmaceutical Sciences, Iwate Medical University, Iwate, Japan.
[b]Present address: Department of Medical Oncology, OITA University Faculty of Medicine, Yufu, Japan
[c]Present address: Medical Oncology, Department of Medicine, Kobe University Hospital and Graduate School of Medicine, Kobe, Japan.
As of October 7, 2007, the novel variations reported here are not found in the database of Japanese Single Nucleotide Polymorphisms (http://snp.ims.u-tokyo.ac.jp/), dbSNP in the National Center for Biotechnology Information (http://www.ncbi.nlm.nih.gov/SNP/), or PharmGKB Database (http://www.pharmgkb.org/).
This study was supported in part by the Program for the Promotion of Fundamental Studies in Health Sciences of the National Institute of Biomedical Innovation, and Health and Labor Sciences Research Grants from the Ministry of Health, Labor and Welfare.